Annu. Rev. Fluid Mech. 2000. 32:203–240

PASSIVE SCALARS IN TURBULENT FLOWS

Z. Warhaft
Sibley School of Mechanical and Aerospace Engineering, Cornell University, Ithaca, New York 14853; e-mail: zw16@cornell.edu

Key Words turbulence, turbulent mixing, temperature fluctuations, small-scale intermittency, anisotropy

■ **Abstract** Passive scalar behavior is important in turbulent mixing, combustion, and pollution and provides impetus for the study of turbulence itself. The conceptual framework of the subject, strongly influenced by the Kolmogorov cascade phenomenology, is undergoing a drastic reinterpretation as empirical evidence shows that local isotropy, both at the inertial and dissipation scales, is violated. New results of the complex morphology of the scalar field are reviewed, and they are related to the intermittency problem. Recent work on other aspects of passive scalar behavior—its spectrum, probability density function, flux, and variance—is also addressed.

1. INTRODUCTION

A passive scalar is a diffusive contaminant in a fluid flow that is present in such low concentration that it has no dynamical effect (such as buoyancy) on the fluid motion itself. A weakly heated flow, such as an air jet, exhibits passive scalar mixing as the cooler air is entrained from the surroundings. Moisture mixing in air and dye in water provide other typical examples. When two chemicals are independently introduced into a fluid, turbulence provides the efficient mixing that enables the reactions or combustion to occur at the molecular level. An understanding of passive scalar behavior is a necessary first step in understanding these processes. The subject of flow visualization depends on interpreting how a passive scalar is related to the velocity field itself.

The scope of this review is as follows: Passive scalar fluctuations are introduced into a simple turbulent flow (Figure 1). We ask, what are the statistical characteristics of the scalar, such as its probability density function (pdf) and structure function (or spectrum), and how do the observations relate to theory? We define simple turbulent flows as those that are steady in time and have a single imposed length scale. They fall into two categories: shear flows (jets, wakes, and boundary layers) and shear-free flows (grid-generated turbulence). For laboratory shear flows, the scalar is usually introduced as a whole (e.g. by weakly heating the jet or the wall of the boundary layer), whereas in the atmospheric boundary layer, it is generally introduced from point or area sources. For grid turbulence,

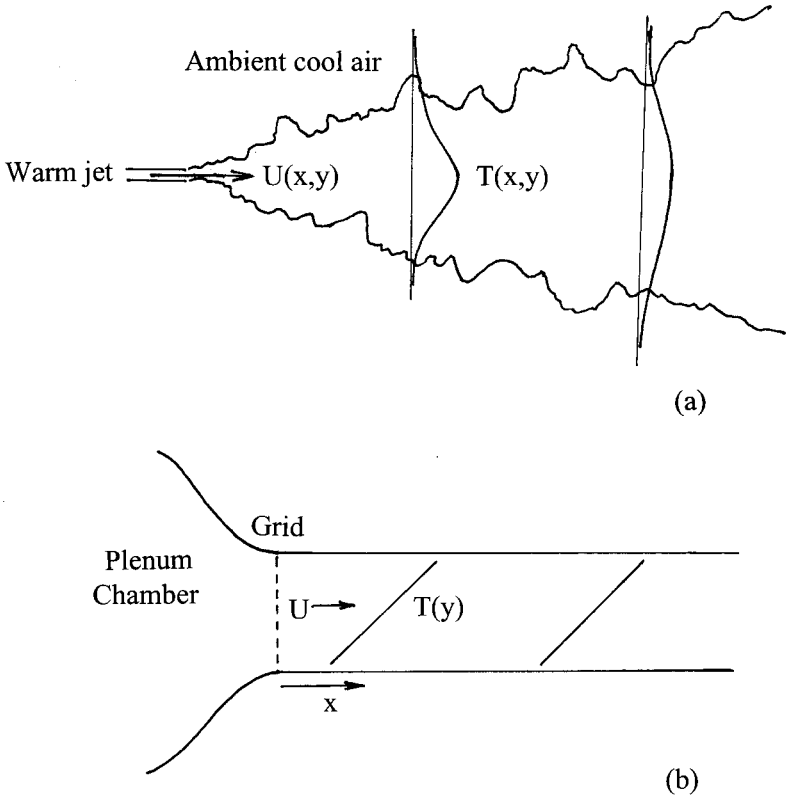

Figure 1 Shear flow (a jet) and grid turbulence. U and T are the mean velocity and temperature respectively, x is the stream-wise direction and y is transverse to it. (a) In the jet, the warm air mixes with the cool ambient air, and scalar fluctuations are produced throughout. (b) Grid-generated turbulence. Here a mean scalar gradient can be produced before the grid in the plenum chamber, and the scalar fluctuations and flux are then produced by the action of the grid. Corrsin (1952) showed, ignoring wall effects, that the mean gradient will sustain itself (with x) because the turbulence is isotropic and there is no flux divergence. Temperature fluctuations without a mean gradient can also be formed by heating the grid or by means of fine wires placed downstream of the grid. In both of these cases the temperature variance decays.

scalar fluctuations may be produced by imposing a mean scalar gradient on the flow. Alternatively, by using an array of finely heated wires in proximity to the grid (or heating the grid itself), fluctuations in the scalar may be achieved without the existence of a mean scalar gradient.

The dynamics of the passive scalar field, Θ, are governed by the convection-diffusion equation

$$\partial\Theta/\partial t + \mathcal{U}_j \partial\Theta/\partial x_j = \kappa\nabla^2\Theta, \quad (1)$$

where κ is the diffusivity and $\mathcal{U}_j$ is the velocity [and repeated indices imply summation: $j = 1, 2, 3$ are the velocity components in the x (streamwise), y, and z directions, respectively]. For much of this review, we have in mind temperature as the scalar, and thus κ is the thermal diffusivity, but the formalism applies to any other passive scalar. Equation 1 is linear in Θ, and thus it may be thought that the scalar problem would be a footnote to the turbulence problem (i.e. the velocity field) itself. The accumulated knowledge over the past 30 years has shown this to be far from the case. Indeed, much of this review is devoted to showing that the cherished paradigms for the velocity field often fail when applied to the scalar.

There has tended to be a certain division between the way engineers and physicists approach the subject. The engineers' interest is in the transport and mixing properties of the scalar, and from this perspective, the focus has been in determining how the variance and flux (integral-scale properties) vary in space and time within particular flows. These quantities are strongly affected by boundary conditions. The physicists, with their quest for universality, have concentrated on inertial and dissipation scales, the hope being, if the Reynolds (Re) and Peclét (Pe) numbers are high enough, that the small-scale behavior will be independent of the large scales. We address both the large and small scales in this review and argue that this division is artificial and dangerous. The experimental evidence shows that the large and small scales are strongly coupled and that the traditional cascade picture, which promotes the notion of universality, is a crude representation. And if the engineer is going to progress in determining reaction rates, dispersion and mixing, then he or she must focus on the small scales and their morphology, because it is here that the strong departures from simple Gaussian behavior occur. The resulting skewed and intermittent fluctuations play a vital role in effecting the ultimate smearing and mixing at the molecular scale, where reactions and combustion occur.

The most comprehensive review of the passive scalar problem in the past decade is by Sreenivasan (1991). This is devoted mainly to the small-scale scalar anisotropy in shear flows (Section 4 of this review) but provides excellent insight into the scalar problem in general. Scalars are also addressed in parts of the review by Sreenivasan & Antonia (1997), which is mainly devoted to the velocity structure [other recent reviews of the velocity field are by Nelkin (1994), Frisch (1995)]. The reviews by Van Atta (1991) and by Zeldovich et al (1988), the book by Lesieur (1997), and the conference proceedings of Boratav et al (1997) also attend to passive scalars. Descriptions of the formalism of Obukhov-Corrsin scaling and the anomalous scaling problem are in Monin & Yaglom (1975). Most recently the subject has been reviewed from a theoretical viewpoint by Shraiman & Siggia (1999). Their review complements the experimental perspective of the present work (particularly Sections 4 and 5).

The review is organized as follows. In Section 2 we briefly outline the traditional phenomenology. In Section 3 we provide recent results on the scalar spectrum. In Section 4 we show that the scalar fluctuations, even at the smallest scales, are anisotropic, in violation of the generally accepted return-to-isotropy picture. We review recent advances in describing the morphology of the scalar field in both the dissipation and inertial subranges, focusing on third-order statistics. In Section 5 we extend this discussion to higher-order statistics. In Section 6 we examine the fluctuating scalar itself by looking at its pdf as well as the covariance and scalar fluxes. Finally, in Section 7 we look at passive scalars for which the Prandtl (or Schmidt) number is significantly different from unity.

2. SOME PRELIMINARIES CONCERNING PHENOMENOLOGY

The scalar and velocity fields may be decomposed into mean and fluctuating components, $\Theta = T + \theta$ and $\mathcal{U}_i = U_i + u_i$. Typical time series of u and θ and their time derivatives are shown in Figure 2. In many problems, determining the scalar variance, $\langle\theta^2\rangle$, flux, $\langle\theta u_j\rangle$, and mean scalar dissipation rate, $\langle\varepsilon_\theta\rangle$ (defined below), are of prime importance. This inevitably leads to an investigation of the statistical nature of θ and ε_θ themselves.

At the outset, scalar phenomenology was based on the Kolmogorov 1941 hypothesis (Monin & Yaglom 1975, Frisch 1995). Thus Obukhov (1949) and Corrsin (1951) argued that, at high Re and Pe [$\mathrm{Pe} \equiv (\nu/\kappa)R_\ell$, where $R_\ell \equiv \langle u^2\rangle^{1/2}\ell/\nu$], there will be a cascade to small scales, where the scalar field will become locally isotropic. Although we show in Section 4 that, in fact, the dissipation and inertial scales are anisotropic (reflecting the large-scale structure), it would be perverse to neglect the scaling that results from the Kolmogorov-Obukhov-Corrsin (KOC) argument. Thus the KOC prediction for the one-dimensional scalar spectrum is

$$F_\theta(k_1) = C_\theta\langle\varepsilon\rangle^{-1/3}\langle\varepsilon_\theta\rangle k_1^{-5/3}, \tag{2}$$

where $\langle\theta^2\rangle = \int_0^\infty F_\theta(k_1)dk_1$, k_1 is the longitudinal wave number, and C_θ is a universal constant. The corresponding relation for the velocity field is

$$F(k_1) = C\langle\varepsilon\rangle^{2/3}k_1^{-5/3}, \tag{3}$$

where C is a universal constant. The issue of the universality of C_θ and C, the applicability of Equations 2 and 3, and what constitutes high Re and Pe are discussed in Section 3.

Both the scalar and velocity fields are observed to exhibit small-scale (internal) intermittency characterized by strong variability in dissipation and mixing rates, and departures from KOC scaling for higher order statistics (Monin & Yaglom 1975, Lesieur 1997, Frisch 1995). As a consequence $\varepsilon = \nu[(\partial u_i/\partial x_j + \partial u_j/\partial x_i)(\partial u_j/\partial x_i)]$

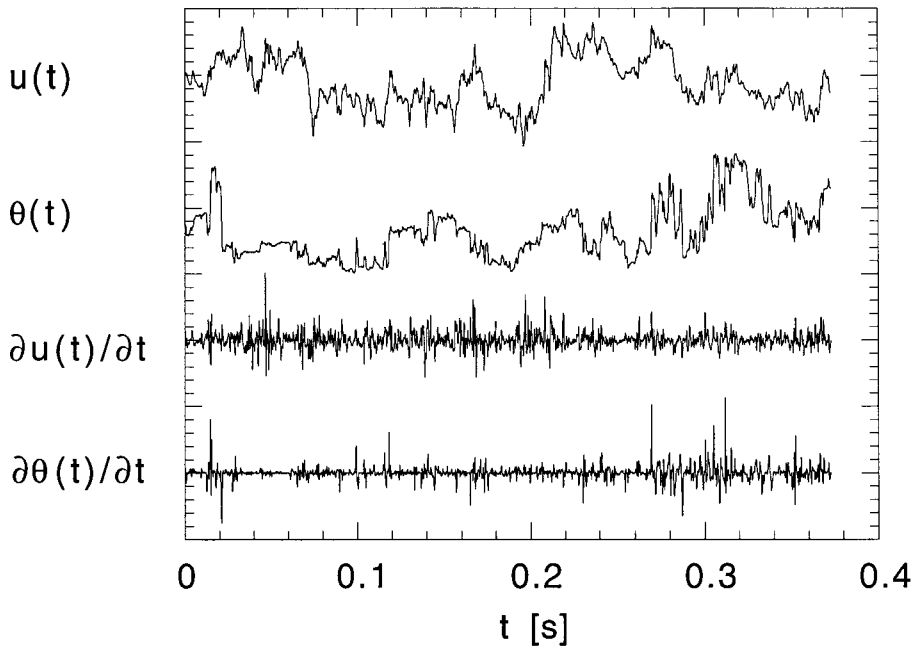

Figure 2 Time-series of the longitudinal velocity fluctuations, u, and the temperature fluctuations, θ, and their derivatives. The flow is grid-generated turbulence with a mean temperature gradient transverse to the flow. The $R_\lambda = 582$, and the kurtosis of $\partial u/\partial t$ and $\partial\theta/\partial t$ are 9.5 and 27.4, respectively [that of $\partial v/\partial t$ (not shown) is 12.2]. The series are taken from the data of Mydlarski & Warhaft (1998a). Similar time series are observed in shear flows (e.g. Meneveau et al 1990).

and $\varepsilon_\theta = 2\kappa(\partial\theta/\partial x_i)(\partial\theta/\partial x_i)$ have non-Gaussian statistics. Much of our evidence of the behavior of ε_θ is based on measurements of $(\partial\theta/\partial t)^2 \sim U^2(\partial\theta/\partial x)^2$, using Taylor's hypothesis (Hinze 1975). $(\partial\theta/\partial t)^2$ is often called the surrogate of $(\partial\theta/\partial x_i)(\partial\theta/\partial x_i)$. The strongly non-Gaussian statistics of $\partial\theta/\partial t$ are evident from Figure 2. Notice the sharper steps in the θ time series than in the u. These give rise to a more intermittent time derivative. This is typical of all turbulent flows with passive scalars. Indeed, it is possible for intermittency in the scalar to occur in a purely Gaussian velocity field (Kraichnan 1994, Holzer & Siggia 1994, and Section 5).

The pdf of the $\partial\theta/\partial t$ with its characteristic stretched exponential tails is shown in Figure 3a. Moreover, as for the velocity field (Sreenivasan & Antonia 1997, Nelkin 1994), the non-Gaussian behavior extends to scales that are larger than the dissipation scale, $\eta \equiv (\nu^3/\langle\varepsilon\rangle)^{1/4}$. Thus scalar differences, $\Delta\theta(r) = \theta(r) - \theta(0)$, for $\ell_\theta > r > \eta_\theta$ are nonGaussian and intermittency is observed at inertial range scales as well as at the dissipation scales. (η_θ is the scalar dissipation scale. The situation in which η_θ is significantly different from η is discussed in Section

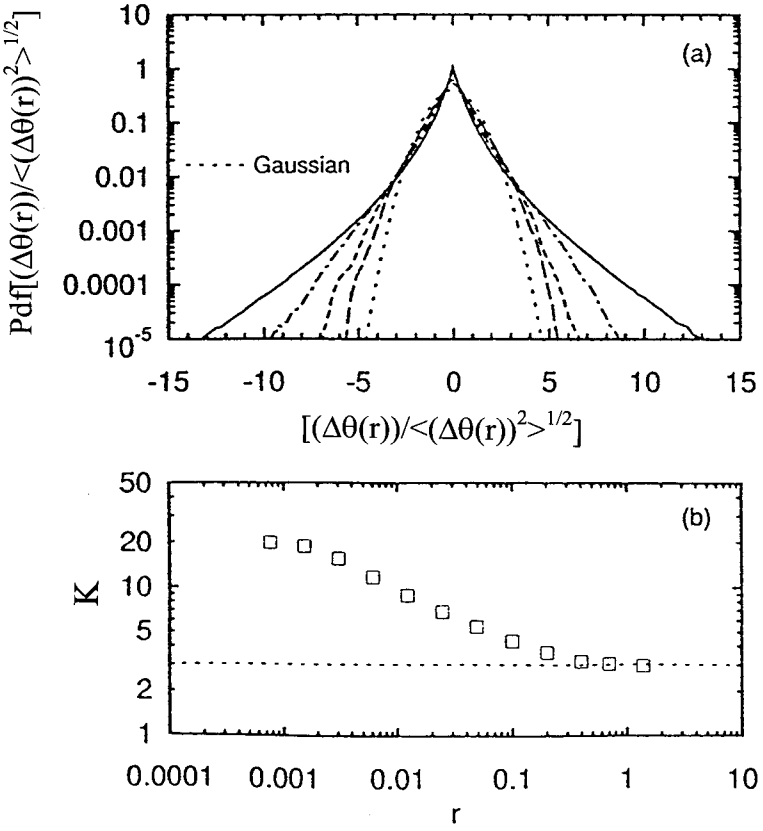

Figure 3 (a) The probability density function (*pdf*) of the passive scalar difference $\Delta\theta(r)/\langle[\Delta\theta(r)]^2\rangle^{1/2}$ as a function of r within the inertial subrange. The *solid curve* is the derivative pdf ($r \sim \eta$) and as r increases the curves tend towards Gaussian. (b) The kurtosis, K, of the scalar difference as a function of r for the same data as for (a). For the smallest r this is the derivative kurtosis. (For this figure r is normalized by the integral scale.) Both (a) and (b) are from the direct numerical simulations of Chen & Kraichnan (1998) using a white-noise velocity field. [For these statistics white-noise computations compare well with laboratory measurements, reproducing similar values of K at the same R_λ (see for example Mydlarski & Warhaft 1998a). In Section 5 we describe results where the white-noise simulations show significant differences to laboratory measurements.] (c) The variation of the kurtosis of the temperature derivative as a function of R_λ. The *plus signs* are the shear-flow data compiled in figure 8 of Sreenivasan & Antonia 1997. The lower R_λ data are from the recent grid turbulence measurements of Mydlarski & Warhaft (1998a) (see their Figure 23b), and Tong & Warhaft 1994 (see their figure 8a). *Circles* are the longitudinal derivative, and *squares* are the transverse derivative (along the temperature gradient). (For data concerning the kurtosis of the velocity field, see Sreenivasan & Antonia 1997).

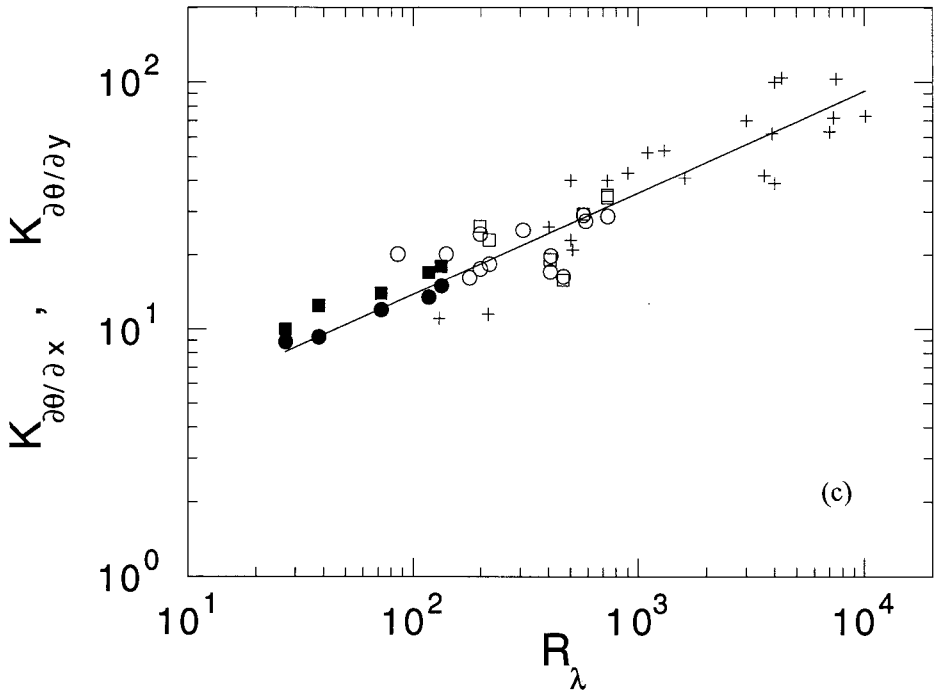

Figure 3 Continued

7.) Figure 3a also shows how the pdf varies with r, and Figure 3b shows the kurtosis of the temperature difference $K_{\Delta\theta}(r)$, defined as

$$K_{\Delta\theta}(r) \equiv \langle \Delta\theta(r)^4 \rangle / \langle \Delta\theta(r)^2 \rangle^2. \quad (4)$$

It tends to the Gaussian value (of 3) at only large scales. As the Re increases, the kurtosis increases too (Figure 3c). Clearly, a full description of the scalar statistics requires information of the higher-order moments. Traditionally, structure functions (rather than spectra) have been used. They are defined as $\langle \Delta\theta(r)^n \rangle$, where n is a positive integer. The difference may be taken in any direction (e.g. along or transverse to the gradient), and it will be shown that the direction plays an important role. (Similarly, higher-order structure functions have been defined, and much more studied, for the velocity field that has qualitative similarities with the scalar) (Sreenivasan & Antonia 1997, Nelkin 1994, L'vov & Procaccia 1997).

KOC scaling ($\langle \Delta\theta(r)^n \rangle = fn\ (\langle \varepsilon \rangle, \langle \varepsilon_\theta \rangle, r)$) implies

$$\langle \Delta\theta(r)^n \rangle \sim r^{n/3}. \quad (5)$$

(For $n = 2$, $\langle \Delta\theta(r)^2 \rangle \sim r^{2/3}$, which Fourier transforms to the $-5/3$ spectrum.) From Equation 5, it follows that $K_{\Delta\theta}$ (Equation 4) is constant (with r), and this is

clearly violated by the measurements (Figure 3b). This is the so-called anomalous scaling problem.

It is important to emphasize that there are apparently two distinct aspects absent from the KOC phenomenology—the departure from local isotropy at the small scales and the internal intermittency. It is one of the objectives of this review to show that they are intimately related.

To cope with the intermittency and thus the non-Gaussian statistics for the velocity field, Kolmogorov (1962) and Obukhov (1962) introduced the integral scale as an added parameter in the scaling of the structure functions. In analogy with the velocity field, the n^{th}-order scalar structure functions now scale as

$$\langle \Delta\theta(r)^n \rangle \sim (r/\ell)^{\zeta_n}. \tag{6}$$

(To see the scaling anomaly, Equation 6 may be written as $\langle \Delta\theta(r)^n \rangle \sim r^{n/3}(r/\ell)^{-\delta_n}$, where $(r/\ell)^{-\delta_n}$ is the departure from KOC scaling.) Realizability conditions (Frisch 1995, Kraichnan 1994) require that $d\zeta_n/dn$ be a nonincreasing function of n (for KOC scaling, it is constant). Notice that $K_{\Delta\theta}$ (Equation 4) accordingly scales as $(r/\ell)^{\zeta_4 - 2\zeta_2}$. Its experimental form (Figure 3b) indicates $2\zeta_2 > \zeta_4$, consistent with the realizability condition. Predicting ζ_n has become a central preoccupation in recent years, and we return to it in Section 5, in which we also elaborate on other aspects of scalar intermittency. Here we note that the above scaling is cast in the form of the two-point structure functions, yet a description of higher-order statistics more generally requires multipoints.

Because the inertial-range structure functions are affected by the intermittency, it should be evident that scalar differences $\Delta\theta(r)$ are conditioned by the instantaneous dissipation rate of the scalar. Exploring this dependence is the subject of the refined similarity hypothesis (RSH) for the passive scalar (Korchashkin 1970, Van Atta 1971, Antonia & Van Atta 1975, Stolovitzky et al 1995). (For the RSH for the velocity field itself, see Frisch 1995). Thus it follows (Stolovitzky et al 1995) that

$$V_\theta = \Delta\theta(r)[(r\varepsilon_r)^{1/6}/(r\varepsilon_{\theta r})^{1/2}], \tag{7}$$

where V_θ is a nondimensional stochastic variable, and ε_r and $\varepsilon_{\theta r}$ are the dissipation rates of turbulence energy and scalar variance averaged over a sphere of radius r. The RSH states that, for high Re and Pe, the conditional pdf of V_θ for a given ε_r and $\varepsilon_{\theta r}$ should be universal. Experiments (Stolovitzky et al 1995, Zhu et al 1995) tend to provide support for this hypothesis, showing an approximately Gaussian form for the pdf of V_θ, although Zhu et al (1995) show some flow dependence, with the atmospheric pdf tending to have a slightly broadened tail compared with the Gaussian distribution. Statistics of $\Delta\theta(r)$ conditioned on $r^{1/3}\varepsilon_r^{-1/6}\ \varepsilon_{\theta r}^{1/2}$ show a strong linear dependence on $r^{1/3}\ \varepsilon_r^{-1/6}\ \varepsilon_{\theta r}^{1/2}$, in agreement with the RSH (Zhu et al 1995, Mydlarski & Warhaft 1998a, Stolovitzky et al 1995). Yet Stolovitzky et al (1995) make the important point that RSH for the scalar may not be a sensitive test of universality of the scalar, because other statistics of the scalar [such as the derivative skewness (see Section 4)] show distinct

departures. They suspect that the process of taking the conditional expectations masks departures from universality.

Finally, it is important that there is one exact, model-independent result. It is for the scalar-mixed moment at high Pe and Re

$$\langle [u(r)][\Delta\theta(r)]^2 \rangle = -(4/3)\langle \varepsilon_\theta \rangle r. \quad (8)$$

This equation, from Yaglom (1949), is the scalar equivalent to the Kolmogorov 4/5 law, $\langle [\Delta u(r)]^3 \rangle = -(4/5) r \langle \varepsilon \rangle$. As for the 4/5 law (Frisch 1995), its derivation assumes global homogeneity. In the wind tunnel (Mydlarski & Warhaft 1998a), Equation 8 appears to be reasonably well obeyed for $R_\lambda > 400$. Chambers & Antonia (1984) also obtain good agreement in the atmospheric boundary layer. Boratav & Pelz (1998) numerically study the higher-order mixed-velocity and -temperature structure functions. Their analysis suggests that there may be an enhanced scaling anomaly for the higher-order mixed moments.

3. THE SPECTRUM OF THE PASSIVE SCALAR FLUCTUATIONS

Sreenivasan (1996) has compiled data of the scalar spectrum slope at various Re for shear flows. This is redrawn in Figure 4. Apparently, the $-5/3$ spectrum is approached when $R_\lambda \sim 10^3 - 10^4$. Here we define the Reynolds number in terms of the Taylor microscale; that is, $R_\lambda \equiv \langle u^2 \rangle^{1/2} \lambda / \nu$, where λ is defined by $\langle u^2 \rangle = \lambda^2 \langle (\partial u / \partial x)^2 \rangle$. Sreenivasan shows that the transverse velocity spectrum evolves in a similar way to the temperature spectrum, yet the longitudinal velocity (u) has a $-5/3$ slope at very low R_λ ($\sim$50). Here, then, the mystery is why the u component achieves the high Re limit at such low R_λ.

The second-order structure function is the Fourier transform of the spectrum, yet measurements in shear flows (Antonia et al 1984, Ruiz-Chavarria et al 1996) indicate a scaling range of 2/3 (corresponding to a $-5/3$ spectrum), for moderate Re in conflict with the spectrum observations (Figure 4). The reason for this is unclear, but apparently stems from the Fourier transform itself. A spectrum bump (bottleneck phenomenon) is observed at high wave numbers, just before the dissipation range (Champagne 1978, Mestayer 1982, Tatarskii et al 1992, Mydlarski & Warhaft 1998a]. It is possible that, at low and moderate R_λ, this bump affects the whole spectrum, deceptively indicating a lower spectrum slope than 5/3. Why this is not reflected in the structure function is unclear, although insight into this in terms of bottleneck phenomena has recently been provided by Lohse & Müller-Groeling (1996) for the velocity field. The issue, which is essentially analytic, requires further attention. Its resolution may change the picture displayed in Figure 4.

Although very high R_λ is required before the $-5/3$ temperature spectrum is observed in shear flows, the opposite is observed in isotropic-grid-generated

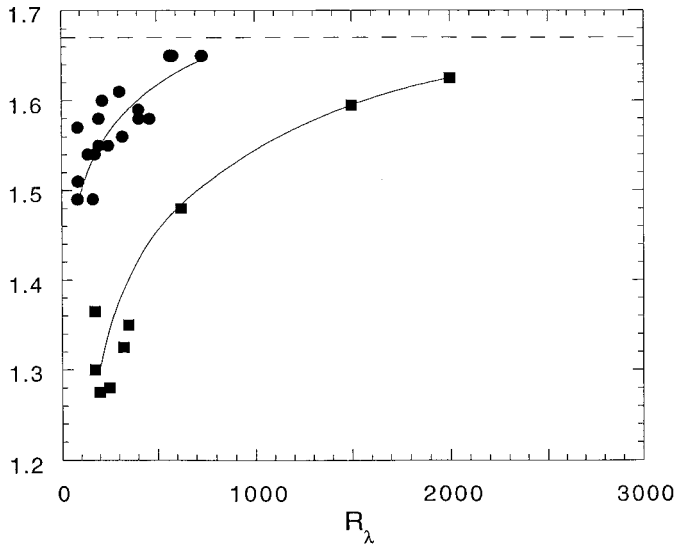

Figure 4 The variation in the spectral slope for various passive scalar spectra as a function of R_λ. For shear flows (*filled squares*), there is a slow evolution toward 5/3, which appears to be approached at large R_λ (>2000). The *filled circles* are the spectral slopes for grid turbulence experiments (no shear). They are close to 5/3 even at very low R_λ. The shear-flow graph is from Sreenivasan 1996 (see also Sreenivasan 1991). The grid turbulence results are from Mydlarski & Warhaft 1998a.

(shearless) turbulence (Figure 4). At very low R_λ, there is a well-developed scaling range, close to $-5/3$ (Yeh & Van Atta 1973, Warhaft & Lumley 1978, Jayesh et al 1994, Mydlarski & Warhaft 1998a), whereas there appears to be none at all for the velocity field [or at most a small range of slope around -1.3 (Jayesh et al 1994)]. For this flow without mean strain, the mere existence of a multiplicity of scales is apparently enough to produce the $-5/3$ scalar spectrum. We see later that many other observed characteristics of the scalar are independent of the details of the velocity field (and its Re), a point recognized early by Kraichnan (1968).

To determine the Obukhov-Corrsin constant C_θ, $\langle \varepsilon_\theta \rangle$ must be estimated. If the small-scale temperature field is isotropic, then $\langle (\partial\theta/\partial x)^2 \rangle = \langle (\partial\theta/\partial y)^2 \rangle = \langle (\partial\theta/\partial z)^2 \rangle$. Yet a number of workers (Budwig et al 1985, Thoroddsen & Van Atta 1996, Tong & Warhaft 1994 in grid turbulence, and Sreenivasan et al 1977 in shear flow) find that $\langle (\partial\theta/\partial y)^2 \rangle \sim 1.4\langle (\partial\theta/\partial x)^2 \rangle$, where y is in the direction of the mean gradient. For grid turbulence, this small-scale anisotropy at the second order appears to be independent of R_λ (Mydlarski & Warhaft 1998a), but all measurements have been done by using similar techniques (using spaced wires), and the result, which is important, requires checking by other means. In an extensive literature survey, Sreenivasan (1996), assuming isotropy, estimates C_θ to fall in

the region 0.3–0.5, with much scatter. For shear flows he uses only high-Re-number atmospheric data, because (Figure 4) a $-5/3$ spectrum, is not observed at low R_λ, and so C_θ (Equation 2) is not defined. His estimate of C_θ for grid turbulence at low R_λ is also in the same range. More recently, Mydlarski & Warhaft (1998a) estimate C_θ to be in the range 0.45–0.55 over a large range of R_λ, using an active grid. They take into account the measured anisotropy. The value of the Kolmogorov constant C (Equation 3) is also $\sim$0.5 for a large class of flows and Re (Sreenivasan 1995), at least for $R_\lambda \geq 200$.

The above results indicate that, even for the very highest Re that can be generated in the laboratory or in the atmosphere and oceans, the scalar spectrum is determined by more than ε_θ, ε, and k. Boundary conditions play an important role, with shear flows behaving quite differently from nonshear flows. The observation that, for grid turbulence, a $-5/3$ scalar spectrum is observed at a low Re in the absence of scaling in the velocity field is particularly intriguing. Finally, internal intermittency, according to Kolmogorov (1962) phenomenology, should affect the slope of the scalar spectrum. As for the velocity spectrum (Nelkin 1994), its effect should be too small to observe experimentally.

4. THE BREAKDOWN OF THE CLASSICAL PHENOMENOLOGY: THE ISSUE OF LOCAL ISOTROPY

The central assumption in KOC scaling is that, at small scales, the scalar (and velocity) field is isotropic in the limit of infinite Re and Pe. Isotropy is also implicit in the intermittency corrections to the simple scaling theory. In Section 3 we indicated that this assumption may be violated at the second order, although the departure from isotropy is relatively small. Here we show that, at the third order, the local isotropy assumption breaks down entirely and that the large-scale behavior of the scalar is directly reflected at the inertial and dissipation scales.

The first cautions appeared over 30 years ago, when Stewart (1969), reporting high-Re-scalar measurements in the atmospheric boundary layer (ABL), showed that the scalar derivative skewness

$$S_{\partial\theta/\partial x} \equiv \langle(\partial\theta/\partial x)^3\rangle/\langle(\partial\theta/\partial x)^2\rangle^{3/2} \tag{9}$$

was of the order one and not zero, which is required for local isotropy in the limit of high Re. [Conventional scaling arguments (see below) indicate $S_{\partial\theta/\partial x} \sim R_\lambda^{-1}$. Atmospheric measurements are in the range $R_\lambda \sim 10^3 - 10^4$]. Since then there has been a constant stream of experimental papers, both in the atmosphere and laboratory, showing the lack of scalar isotropy at both the dissipation and inertial scales. The earlier papers focused on the derivative skewness (Gibson et al 1970, Freymuth & Uberoi 1971) and the problems of possible probe contamination (Wyngaard 1971, Mestayer et al 1976). By the late 1970s it was clear that the effect was real and ubiquitous. Traces of the scalar signal (Figure 5a) showed

characteristic ramp-cliff structures (Gibson et al 1977, Sreenivasan & Antonia 1977, Mestayer et al 1976, Sreenivasan et al 1979). The magnitude of the skewness caused by these structures appears to be independent of Re although a systematic study for specific shear flows is still needed (see Sreenivasan 1991 for a summary of data from shear flows; grid flows are discussed below). An analysis of the temperature structure functions, by Van Atta (1971) and by Antonia & Van Atta (1978) for the ABL and for a heated jet, showed that the odd-order structure functions (which should vanish at high Re if the scalar field is isotropic) have clear scaling ranges, indicating that the anisotropy is not confined to the dissipation ranges.

All of the above measurements were for external flows that contain large-scale intermittency (caused by excursions of ambient air entraining the fluid) as well

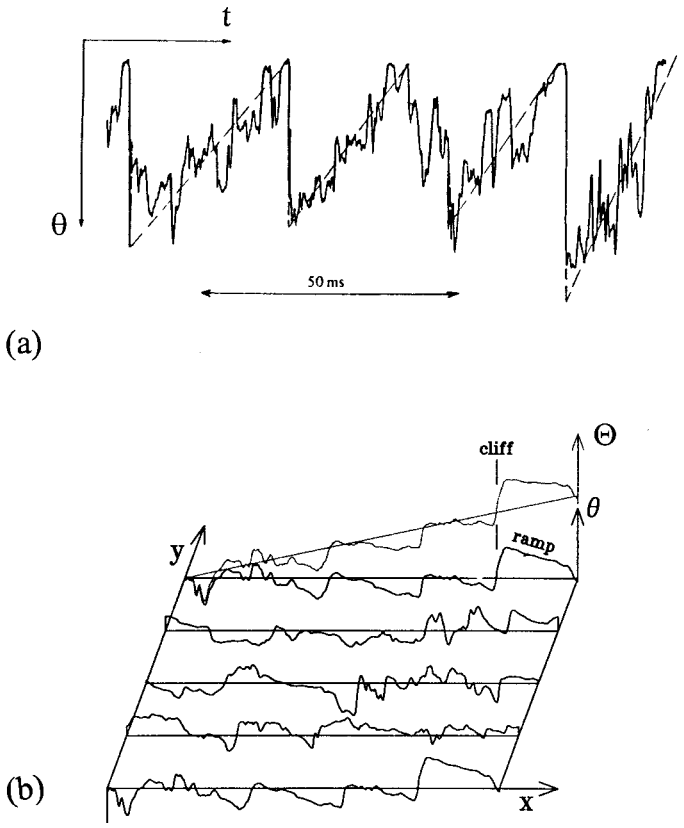

Figure 5 (a) A time series of temperature in a heated jet showing the ramp-cliff structure, from Sreenivasan et. al (1979). (b) Temperature spatial variation from numerical simulations of Holzer & Siggia (1994) with a mean temperature gradient. The full scalar is the top trace. The other traces are of the fluctuating component only.

as internal intermittency. Any lingering doubt that the structures were caused by the complexity of these shear flows was dispelled by grid turbulence measurements (Tavoularis & Corrsin 1981b, Budwig et al 1985, Tong & Warhaft 1994) and the numerical simulations of Pumir (1994). Here, too, the derivative skewness was observed along the mean gradient despite the absence of entrainment and large-scale velocity anisotropy. Even more remarkably, the same ramp-cliff structures were observed in numerical simulations of Holzer & Siggia (1994) (Figure 5b). Here the turbulence was two dimensional and Gaussian, with none of the fine scale structure observed in real turbulence. Apparently only a multiplicity of scales, acting against an imposed mean temperature gradient, is all that is required to obtain the persistent anisotropy.

Insight into the ramp-cliff structures was achieved by mapping, in a plane jet, the isocontours of velocity and temperature (Antonia et al 1986). Large-scale velocity structures (or eddies) form converging and diverging separatrix and saddle points (Figure 6a). These must occur in all flows, but in shear flows they are inclined, on average, along the same direction as the principle strain (at $\sim 40^\circ$ for a jet). If a passive scalar field is formed in the flow, a temperature front will occur at the diverging separatrix. The front demarks the cool and warm fluids entrained by the two counterflowing structures (Antonia et al 1986). While the ramp-cliff structures are large-scale features, on the order of an integral scale (e.g. Gibson et al 1977), the front itself is sharp, and thus is manifested at the small scales. Tong & Warhaft (1994) showed that, as the Re increases, the fronts become sharper and more intense, occurring deeper in the tails of the pdf. It is this combination of large- and small-scale characteristics that provides the challenge to simple scaling.

All turbulent flows, be they with or without shear, must contain large eddies. In the no-shear case, the saddle points are randomly oriented. However, if a mean temperature gradient is applied to the flow, the diverging-converging separatrices that happen to be aligned with the mean gradient cause ramp-cliff structures. This is clearly shown in the numerical simulations of Holzer & Siggia (1994). The stream functions (Figure 6b) are similar in character to those observed in the shear flow (Figure 6a). A temperature front (Figure 6c) forms at the diverging separatrix. We surmise that had we not been imbued with the Kolmogorov phenomenology, the above picture of a fundamentally anisotropic scalar field would seem natural. We would expect that, as the large eddies act on the scalar gradient, large discontinuities might occur. It is the very strong attraction to universality that has diverted our attention.

Since Sreenivasan's 1991 review, which is mainly devoted to the derivative (rather than inertial-scale) anisotropy in shear flows, there have been developments, theoretical, numerical, and experimental, for the inertial and dissipation ranges for the simple situation of a linear temperature profile in isotropic grid turbulence (Figure 1b), which we now outline.

First it is important to emphasize that in this flow, because of symmetry, any odd moments in x must be zero, and this has been observed (e.g. Tong & Warhaft

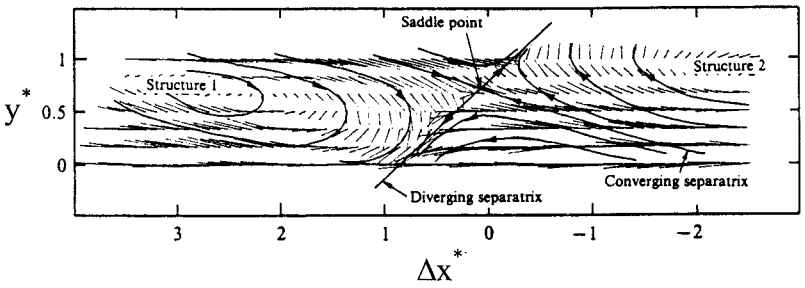

(a)

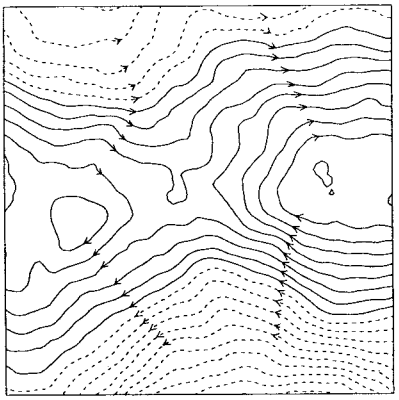

(b)

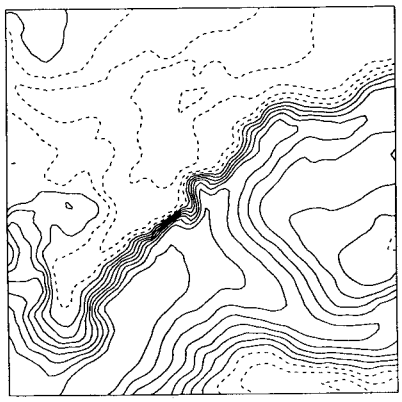

(c)

Figure 6 (a) The diverging-converging velocity separatrix of the plane jet of Antonia et al (1986) (the observer is traveling at the convection velocity). (b) The stream functions from numerical simulations of Holzer & Siggia (1994) show the same pattern, but unlike the jet, this pattern is directionally unconstrained because the turbulence is isotropic (no shear). (c) Temperature isocontours in the same flow as b, showing the cliff along the saddle point. The mean scalar gradient is in the *x* (horizontal) direction.

1994, Tavoularis & Corrsin 1981b). The local-isotropy hypothesis also requires that these moments in the *y* direction (Figure 1b) must be zero, but this is not the case, because of the very existence of the ramp-cliff structures. We also note that, in shear flows (Figure 1a) odd-order moments are nonzero in both the *x* and *y* directions. Thus, in heated shear flows, a single probe will measure ramps and cliffs, but it requires an array (in the *y* direction) to observe them in the linear-temperature-profile case. Note that, in the *x* time series of Figure 2, the ramp-cliffs are not in evidence because of this. [There is, however, a low probability that a ramp-cliff may occur transverse to the gradient (see Tong & Warhaft 1994,

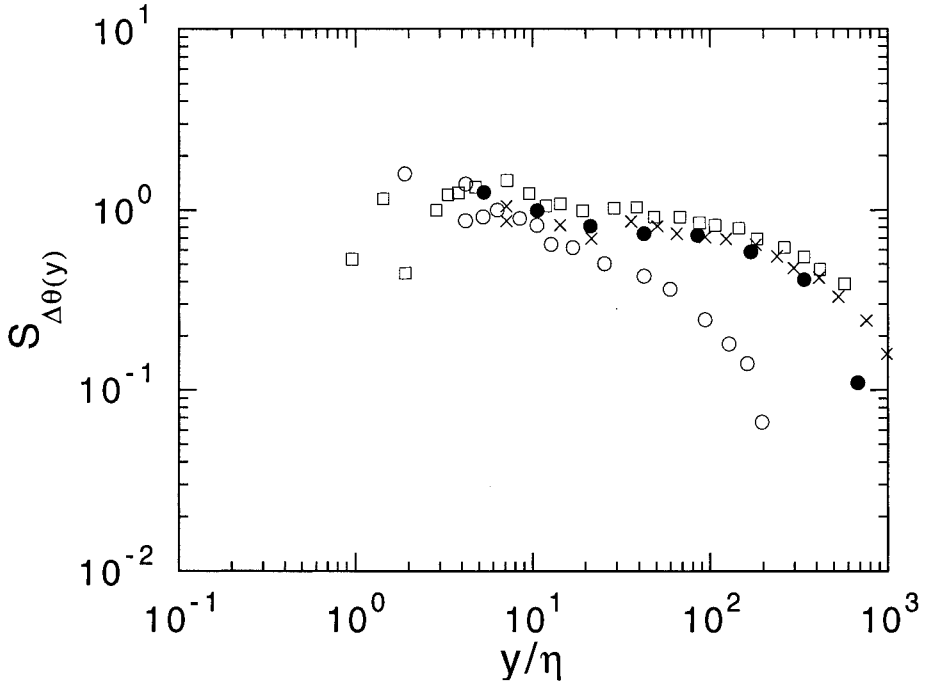

Figure 7 The skewness structure function $S_{\Delta\theta(y)} \equiv \langle[\Delta\theta(y)]^3\rangle/\langle[\Delta\theta(y)]^2\rangle^{3/2}$ as a function of y/η for grid turbulence with a linear temperature gradient in the y direction (from Mydlarski & Warhaft 1998a). *Open circles, squares, filled circles,* and *crosses* are R_λ = 99, 222, 247, and 461, respectively. Notice the plateau for $R_\lambda > 200$.

Figure 7). We show below that, although the preferred direction is along the gradient, their orientation fluctuates].

As for the shear-flow case (Antonia & Van Atta 1978), the third-order structure function exists, with a scaling-range of slope 0.9–1.0 and with little Re dependence (Mydlarski & Warhaft 1998a). Figure 7 shows the normalized third-order structure function (skewness structure function), $S_{\Delta\theta} \equiv \langle\Delta\theta(y)^3\rangle/\langle\Delta\theta(y)^2\rangle^{3/2}$. As R_λ increases, the structure function levels off to a clearly defined plateau. Because the mean gradient is the reason for the existence of $\langle\Delta\theta(y)^3\rangle$, following Lumley (1967) we include it (to the first order) in a Kolmogorov scaling estimate, such that $\langle\Delta\theta(y)^3\rangle \sim \mathrm{d}T/\mathrm{d}y\ fn(\langle\varepsilon\rangle,\langle\varepsilon_\theta\rangle,y)$. This yields $\langle\Delta\theta(y)^3\rangle \sim y^{5/3}$ and $S_{\Delta\theta} \sim y^{2/3}$. Thus the observed ($y$-independent) scaling is in contradiction to the Kolmogorov picture. Note (Figure 7) that for $\Delta/\eta \to 1$, $S_{\Delta\theta} \to S_{\partial\theta/\partial y}$, the derivative skewness. Its value is $\mathcal{O}(1)$ and does not depend on Re. [This is further corroborated by Mydlarski & Warhaft (1998a) for $30 \leq R_\lambda \leq 730$.] Kolmogorov scaling (in the same vein as above) indicates $S_{\partial\theta/\partial y} \sim R_\lambda^{-1}$, that is, the effect of the mean gradient is confined to low Re, in agreement with the return to isotropy principle. The fact

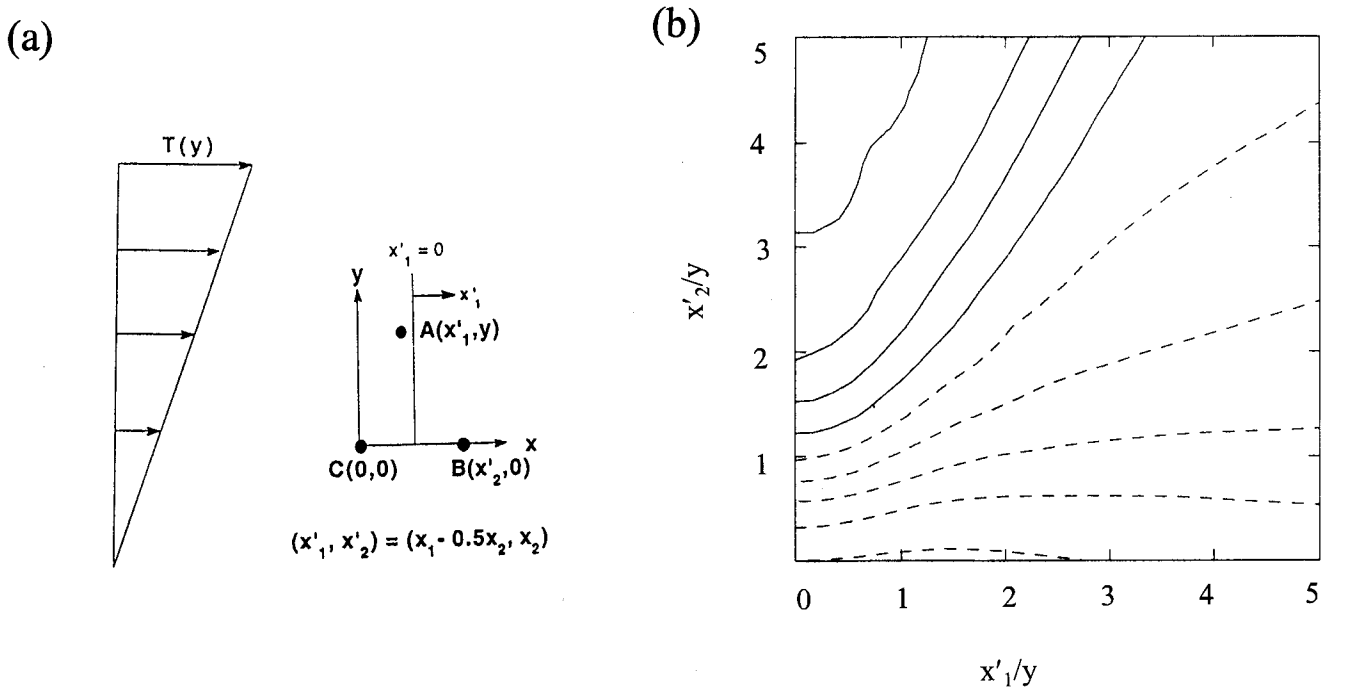

Figure 8 (a) The coordinate system for the three-point correlations. The flow is in the x direction. (b) The contour plot of the three-point triple correlation $\langle\theta_A\theta_B\theta_C\rangle$. The data are normalized by $-\langle\theta_A\theta_B\theta_C\rangle_{0,0}$ at the given transverse separation, which is $y/\ell = 0.051$. Isocontours are separated by 0.2. *Dashed lines* are negative, *solid lines* are positive (the -1 contour is the lowermost dashed line). (From Mydlarski & Warhaft 1998b.)

that $S_{\partial\theta//\partial y}$ does not change with R_λ in either shear or unsheared flows indicates that the return-to-isotropy principle is fundamentally flawed.

Traditional two-point statistics will not reveal the morphology of the scalar field, and we turn to a three-point description. We first describe experiments and then relate them to the theory. We are interested in seeing how the anisotropy is manifested in the inertial (rather than the dissipation) range, and thus we require a relatively high Re. The active grid (Mydlarski & Warhaft 1996) provides this range ($200 < R_\lambda < 500$).

Figure 8 shows the three-point triple correlation $\langle\theta_A\theta_B\theta_C\rangle$. Obtaining this function from the two probes (using Taylor's hypothesis and differencing techniques) is not trivial, and it is described by Mydlarski & Warhaft (1998b). Known symmetry properties were imposed: the statistics must be even in x and odd in y. In addition, because the function is even in x and x_1', only the positive quadrant ($x'_{1\,\mathrm{and}\,2}/y > 0$) needs to be displayed. The nondimensionalization is by $-\langle\theta_A\theta_B\theta_C\rangle|_{x_1'=0,x_2'=0}$ and hence, for $(x_1', x_2') = (0,0)$, the triple correlation is -1. It can also be shown that $\langle\theta_A\theta_B\theta_C\rangle$, because of the symmetries, must be zero when the three points form an equilateral triangle (Pumir 1998). This occurs when $(x_1'/y, x_2'/y) = (0, 2/\sqrt{3})$.

For $x_1'/y = x_2'/y = 0$, the triple correlation reduces to the third-order transverse the three-point correlation function for a particular y value. The condition $x_2'/y = 0$, with x_1'/y increasing, yields the diagonal two-point correlation. It remains close to unity, indicating that the x dependency on the ramp-cliff structures (mainly oriented in the y direction) is relatively weak (Mydlarski & Warhaft 1998a,b). As B moves from C (increasing x_2'/y with x_1'/y fixed), the chance of both of these points falling on the same side of a front (or cliff) diminishes. Thus the magnitude of $\langle\theta_A\theta_B\theta_C\rangle$ diminishes. Its decrease is most rapid for $x_1'/y = 0$, because here the triangle is always iscoceles. On the other hand, consider $x_2'/y =$ constant ($\neq 0$) with x_1'/y increasing. Here we would expect the magnitude of the correlation to increase because, for $x_1'/x_2' \gg 1$, the triple correlation tends to the two-point, third-order diagonal correlation. The curves of Figure 8 confirm this. [The peeling off (at large x_1'/y) is apparently caused by the finite inertial range.] The picture shown in Figure 8 is robust both in terms of the Re and inertial-range spacing (Mydlarski & Warhaft 1998b).

The above measurement was motivated by the theoretical work of Shraiman & Siggia (1995, 1996) and Pumir (1996a, 1997, 1998). They consider the Hopf equation, which describes the multipoint correlators of the scalar. For white noise it can be shown (Chertkov et al 1995, Gawedzki & Kupiainen 1995, Shraiman & Siggia 1995) that lower-order correlators act as source terms for higher-order ones and that there is a formal connection to Kolmogorov scaling. Shraiman & Siggia (1995, 1996), recognizing, however, that white noise does not produce the observed scaling for the third-order structure function (see Section 5), use a more physical velocity field with spatiotemporal correlations. For this case the resulting Hopf equation is phenomenological and contains a free parameter. They argue that the correlator (from the Hopf equation) is highly symmetric and is integrable

by using Lie algebraic methods. Their computed results (Pumir 1997, 1998) yield correct scaling for the third-order (two-point) structure function. Their calculated three-point triple correlation is shown in Figure 9. It reproduces the main experimental features of Figure 8.

A white noise model would produce results that are similar to those in Figure 9 since the normalization divides out the dominant effects of its incorrect scaling exponent. The qualitative shape of Figure 9 can also be reproduced using a simple step in the scalar that fluctuates randomly about its orientation along the mean gradient (Mydlarski et al. 1998). Yet as the case for two point statistics, the objective is to develop theory that can quantitatively account for the data.

We are so used to focusing on two-point statistics that it will take time to adjust to three-point statistics, (Figures 8 & 9) which offer more to measure and compute than traditional scaling. We expect that the same features for the scalar field will be observed in shear flows, but it remains to be seen whether there is a significant quantitative difference.

We emphasize that the above results are not pathological, but are inherent in the nature of the way a scalar is mixed. The picture described suggests that the scalar anisotropy should be independent of the details of the turbulence itself (as long as it has a multiplicity of scales). Moreover, the ramp-cliff structures must give rise to higher-order non-Gaussian effects in the scalar field, and this is observed in the Holzer & Siggia (1994) numerics, in which the scalar kurtosis is

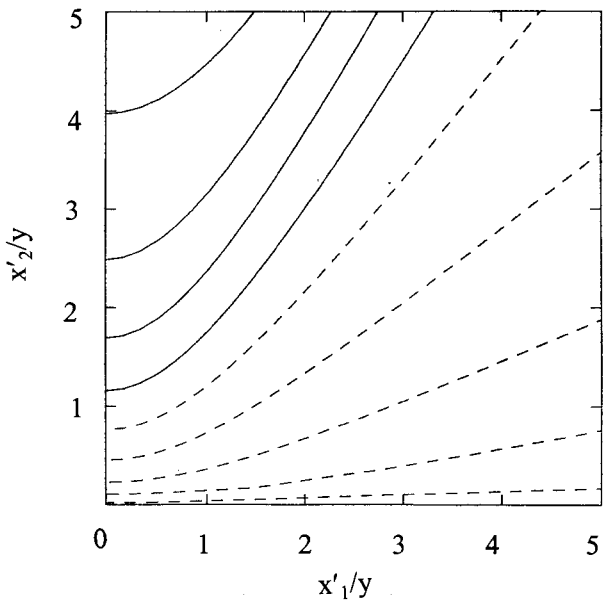

Figure 9 The contour plot of the three-point triple correlation computed from the theory of Pumir, Shraiman, & Siggia. Same range as Figure 8. (From Mydlarski et al 1998).

greater than the Gaussian value of 3, and small-scale intermittency (in the strictly Gaussian velocity field) is observed. We now turn to the issue of the higher-order statistics.

5. HIGHER-ORDER STRUCTURE FUNCTIONS AND INERTIAL SUBRANGE INTERMITTENCY

The anisotropy, manifested in the third-order statistics, is only in evidence when there is a mean scalar gradient. In the absence of a mean gradient, the derivative skewness is zero by symmetry (Budwig et al 1985, Tong & Warhaft 1994). The instantaneous action of the large eddies must still produce sharp discontinuities in an advected scalar field, but they have no preferred orientation (Figure 10) and average to zero in any given direction. These discontinuities give rise to non-Gaussian effects at the small scales, now manifested only in the higher-order even moments. Thus the intermittency issue, outlined in Section 2, is closely related to the anisotropy issue discussed in Section 4. Both result from the persistent effect of the large-scale discontinuities at the small scales.

The velocity field also exhibits small-scale intermittency (Nelkin 1994, Sreenivasan & Antonia 1997), and this intermittency too must be related to the large eddy structure. Although there are phenomenological models that attempt to describe the velocity intermittency, their connection to the Navier-Stokes equation is uncertain. At present it is felt that the scalar problem may be more tractable. The scalar equation is linear. Moreover scalar intermittency occurs in the absence of velocity intermittency (i.e. the velocity field can be strictly Gaussian) as long as there is a multiplicity of scales. The theoretical and numerical work of Kraichnan (1994) and of Holzer & Siggia (1994) show this, as do wind tunnel experiments (see below).

Kraichnan (1968) derived exact results for the scalar field if the velocity field is assumed to have an infinitely rapid decorrelation time (a ''white'' or ''δ-correlated'' velocity field). Exact white-noise equations for the higher-order moments were derived by Kraichnan (unpublished data, 1994) and by Shraiman & Siggia (1994). The consequences of these equations and their relation to KOC scaling were analyzed by Chertkov et al (1995), Gawedski & Kupiainen (1995), and Shraiman & Siggia (1995). In a parallel development Kraichnan (1994), using a linear ansatz, derived a prediction for the higher-order structure-function scaling exponents. This has provided fertile ground for the analysts (see Chen & Kraichnan 1998 for a comprehensive list of recent theoretical and computational work).

The issue is summarized in Figure 11, which is a plot of the scaling exponent of the structure-function $\langle \Delta\theta(r)^n \rangle$ plotted as a function of n. As mentioned in Section 2, KOC scaling (no internal intermittency) implies a linear relation. The experimental and numerical data show a slower than linear increase as a consequence of the internal intermittency. [The velocity scaling exponent of $\langle \Delta u(r)^n \rangle$

Figure 10 A snapshot of the spatial amplitude of an evolved scalar field from the direct numerical simulations of Chen & Kraichnan (1998) using a white noise velocity field. *White* is warm. *Black* is cool. Although the white noise calculations are inconsistent with the scaling exponent for the scalar structure functions determined by experiment (see text), they do capture the qualitative characteristics of the small scale intermittency, and of the ramp-cliff structures (which occur along the lines of demarcation between the warm and cool fluid).

is shown too. It is significantly less intermittent than the scalar, but it too departs markedly from Kolmogorov (1941), at higher orders].

The data in Figure 11 are from various sources and were obtained by various methods. The first reliable data (Antonia et al 1984) are from measurements of the pdf. Deriving the exponents this way or directly from the structure function presents convergence problems, because, as the order increases, the information required resides further into the tails of the pdf. Thus, in principle, very large samples are required. Yet tests carried out in our laboratory show that the scaling

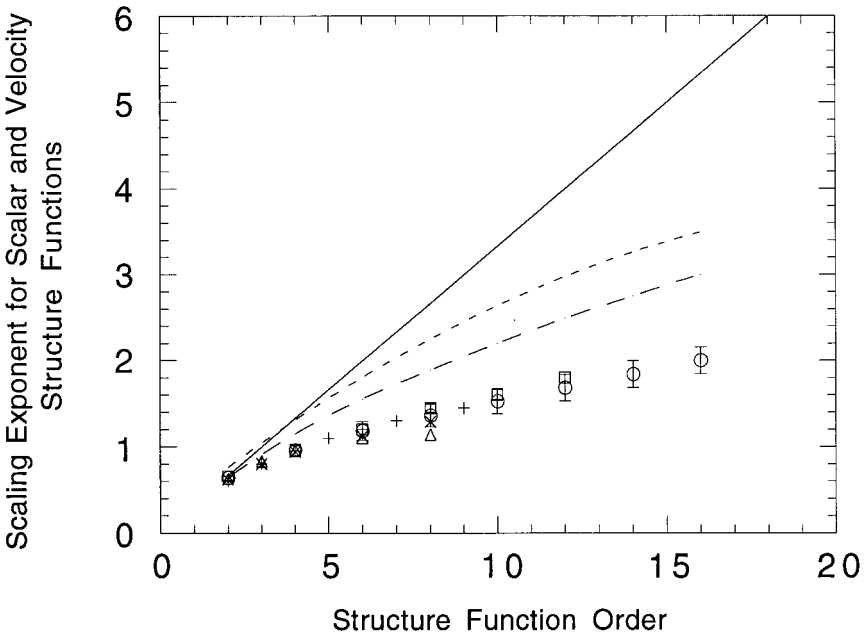

Figure 11 The scaling exponent ζ_n for the scalar structure function $\langle[\Delta\theta(r)]^n\rangle$ within the inertial subrange as a function of *n*. *Squares* are from the data of Antonia et al (1984) (heated jet), *crosses* are from the data of Ruiz-Chavarvia et al (1996) (heated wake), *triangles* are from the data of Meneveau et al (1990) (heated wake), *circles* are from the data of Mydlarski & Warhaft (1998a) (grid turbulence), and *plus signs* are from the full, three dimensional Navier-Stokes numerical simulations of Chen & Kraichnan (1998). *Vertical bars* represent uncertainty for the Mydlarski & Warhaft data. The *long-dashed line* is the white-noise estimate from Kraichnan (1994). *The short-dashed line* is for the velocity field from Anselmet (1984). The solid line is the KOC prediction.

exponent is not strongly affected when shorter reords are used, although the value of the moment changes. (This point was made earlier for the velocity data by Anselmet et al 1984.) The Antonia et al data are consistent with the (Navier-Stokes) Direct Numerical Simulations (DNS) of Chen & Kraichnan (1998), also shown in Figure 11. L. Mydlarski & Z. Warhaft (unpublished data) have analyzed their active grid data and extended the set to order 16. Their data are also consistent with Antonia et al (1984). Ruiz-Chavarria et al (1996) have used a form of extended self similarity to provide a larger scaling range (Benzi et al 1993), and their results lie on the same curve. The data of Meneveau et al (1990), obtained from analysis of experimental data by using joint multifractal formalism, tend to flatten out at $n \sim 6$, suggesting stronger intermittency at higher orders.

The above measurements and computations suggest that the true curve probably lies somewhere between the Antonia et al (1984) curve and that of Meneveau

et al (1990). It would be inconsistent with realizability (see Section 2) if the true curve increases more rapidly than that of Antonia et al, which show an approximately linear increase above order 5 or 6 (we assume that in all data sets the convergence is good below this order). On the other hand the possibility of a slower increase cannot be ruled out.

The Kraichnan (1994) prediction, with the white in-time velocity field and the linear ansatz for the molecular-diffusion terms, is also shown in Figure 11. Although the model (by using a strictly Gaussian velocity field) shows the right trend in the scalar intermittency, it is quantitatively inconsistent with the data. DNS computations with white noise are also inconsistent with the Kraichnan predictions (Frisch et al 1998, Pumir 1998, Chen & Kraichnan 1998). These white-noise DNS computations are also inconsistent with experiments, yielding, for example, the wrong scaling exponent for the third-order structure function (Pumir 1998). Although the white-noise approach provides insight, it is clear that a more realistic velocity field must be used for this problem. Experimental mapping of multipoint correlations for higher-than-third-order functions may provide impetus for further advances. Any comprehensive theory will have to predict these correlations; the two-point correlations of Figure 11 are only scant indicators of the subtle underlying structure.

The internal intermittency can also be quantified in terms of an autocorrelation of ε_θ,

$$\rho_{\varepsilon_\theta \varepsilon_{\theta r}} \equiv \langle \varepsilon_\theta(x)\varepsilon_\theta(x + r)\rangle / \langle \varepsilon_\theta^2 \rangle \sim r^{-\mu_\theta}, \tag{10}$$

where μ_θ is known as the scalar intermittency exponent (Chambers & Antonia 1984, Sreenivasan & Antonia 1997). Making the weak assumption that

$$\langle [\Delta u(r)]^2 [\Delta\theta(r)]^4 \rangle \sim r^2 \langle \varepsilon_\theta(x)\varepsilon_\theta(x + r)\rangle, \tag{11}$$

which is the scalar equivalent to the common assumption (Frisch 1995) that $\langle \Delta u(r)^6 \rangle \sim r^2 \langle \varepsilon(x)\varepsilon(x + r)\rangle$, it follows from Equations 10 and 11 that

$$\langle [\Delta u(r)]^2 [\Delta\theta(r)]^4 \rangle \sim r^{2-\mu_\theta}. \tag{12}$$

Thus μ_θ can be related to the structure function scaling exponents, implying it too has a universal value at high Re and Pe.

Using atmospheric data in the high-Re-number range $R_\lambda \sim 10^3$–10^4, Chambers Antonia (1984) find $\mu_\theta = 0.25 \pm 0.05$. This value is supported by wind tunnel measurements of Mydlarski & Warhaft (1998a), who determine μ_θ over the range $90 \leq R_\lambda \leq 700$. Using multifractal techniques, Prasad et al (1988) and Meneveau et al (1990) determine μ_θ to be somewhat higher, in the range 0.35–0.4. We have noted above (Figure 11) that the multifractal estimate of the scalar structure function exponent also departs from those obtained by using more direct methods. [The value of μ for the velocity field is fairly well established to be $\sim$0.25 (Sreenivasan & Antonia 1997).]

The grid turbulence measurements of μ_θ by Mydlarski & Warhaft (1998a) show little trend with R_λ (Figure 12). At their low R_λ ($\sim$100), $\mu_\theta \sim 0.2$, whereas μ, the

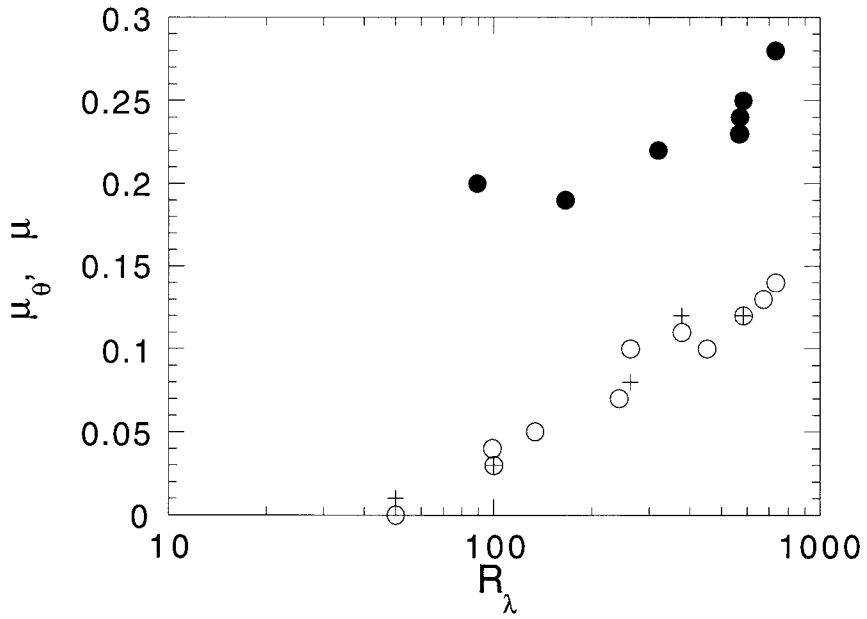

Figure 12 The velocity and scalar-intermittency exponents, μ and μ_θ, respectively, as a function of R_λ. *Open circles* are for μ determined from the autocorrelation of ε^{11} [$\sim \langle(\partial u/\partial t)^2\rangle$]. *Plus signs* are for μ determined from ε^{12} [$\sim \langle(\partial v/\partial t)^2\rangle$]. *Solid circles* are for μ_θ determined from the autocorrelation of ε_θ [$\sim \langle(\partial\theta/\partial t)^2\rangle$]. From Mydlarski & Warhaft (1998a).

intermittency exponent for the velocity, was found to be close to zero (only becoming significant for $R_\lambda > 200$). These results experimentally confirm that inertial subrange intermittency in the scalar can occur in the absence of intermittency in the velocity field (Kraichnan 1994, Holzer & Siggia 1994, Chen & Kraichnan 1998).

6. THE INTEGRAL-SCALE CHARACTERISTICS: THE SCALAR PDF, VARIANCE, COVARIANCE, AND FLUX

Up to this point, we have addressed inertial and dissipation scales. Much research has been devoted to these scales because of the expectation of universality. Although we have shown that, in fact, the integral-scale characteristics cannot be ignored, this should not make the study of the small scales less important. To numerically simulate the scalar (and velocity) field, the inertial and dissipation scales are often modeled (in such schemes as Large Eddy Simulation; Galperin & Orszag 1993), so that the immense volume of data can be managed. Thus there is a practical need for a deep and accurate understanding of the physics of the

small scales, so that their parameterization will be correct. Yet, for the engineer, the integral scales are of particular significance in themselves, because, to estimate transport and mixing, the scalar variance, flux, and covariance, must be known. We now turn to those quantities, beginning with the scalar pdf itself.

6.1 The Scalar pdf

The data in Figure 3a and b show that, as r increases, the kurtosis of the scalar difference approaches the Gaussian value of 3. Earlier measurements of the scalar pdf in homogeneous turbulence (Tavoularis & Corrsin 1981a) also indicated that a Gaussian distribution was a satisfactory model for the scalar signal itself. However, unlike the spectrum and structure function, the pdf did not receive serious attention, presumably because of an implicit (and wrong) assumption that the central limit theorem would constrain the pdf to be Gaussian in homogeneous flows. Yet the Chicago convection experiment (Castaing et al 1989, Siggia 1994), which showed that, under certain conditions, the (nonpassive) scalar pdf had exponential tails, motivated a deeper look at this problem. Notably, Pumir et al (1991) developed a phenomenological mean-field model that showed that, if a passive mean scalar gradient is present, the scalar pdf will have exponential tails. This was cast in more rigorous terms with Lagrangian path integrals by Shraiman and Siggia (1994). The exponential tails are the result of anomalous mixing; they arise from improbable events in which a parcel of fluid moves a distance much greater than the integral-length scale without equilibrating. Shraiman & Siggia (1994) show that this occurs for a typical fluid path for which the mixing rate is anomously long rather than for a typical mixing rate but with an atypical path.

The Pumir, Shraiman, & Siggia (PSS) prediction gave rise to a spate of papers; theoretical, experimental, and numerical. Holzer & Pumir (1993) derived the PSS theory by using the Kerstein (1991) linear eddy model, which describes turbulent mixing as a collection of instantaneous local rearrangements of the scalar followed by diffusion. They also implemented the Kerstein model numerically and found nearly exponential tails in the presence of an imposed linear mean-scalar gradient. Kerstein & McMurtry (1994) generalized the mean-field analysis of Holzer & Pumir (1993) and also used the Langevin equation to represent the concentration time history within a fluid element. They found general agreement with PSS but argue that PSS makes restrictive modeling assumptions. They suggest a wider possible range of pdf tails. Earlier, Sinai & Yakhot (1989) had deduced an exact closed-form solution for the scalar pdf equation with no mean gradient. They showed that the pdf is determined by the conditional expectation of the scalar dissipation rate. This result was generalized by Pope & Ching (1993), who showed that the pdf of any stationary process can be obtained exactly from the conditional expectations of time derivatives of the same signal. Although providing a connection, these formal results do not solve the problem. Further discussions about the conditional dependence between the scalar and its dissipation can be found in work by O'Brien & Jiang (1991), Sahay & O'Brien (1993),

Eswaran & Pope (1988), Mi & Antonia (1995), Jayesh & Warhaft (1992), and Anselmet et al (1994).

The experimental evidence is as follows. Gollub et al (1991) and Jayesh & Warhaft (1991) (see also Lane et al 1993 and Jayesh & Warhaft 1992), showed that, in grid-generated turbulence, there are clear exponential tails in the presence of a mean gradient (Figure 13). The turbulence-generating mechanisms and measurement techniques were quite different in the two experiments. In the Gollub et al (1991) experiment, an oscillating grid (in water and in water glycerol mixtures) was located between constant-temperature, hot and cold oil baths, which provided the mean temperature gradient. In the Jayesh & Warhaft (1991) experiment, a conventional grid was used, with the air differentially heated (to form the linear temperature gradient) in the tunnel plenum (Sirivat & Warhaft 1983). Jayesh & Warhaft (1991, 1992) verified that the velocity field itself was Gaussian. They also showed that, in the absence of a mean gradient or when the scalar gradient was symmetric but nonlinear (a thermal mixing layer with an error function profile; Ma & Warhaft 1986), the pdf of the scalar did not exhibit exponential tails (in fact, for the thermal-mixing layer, it was slightly sub-Gaussian). These experiments corroborate the PSS theory.

Both in the Gollub et al (1991) and Jayesh & Warhaft (1991) experiments, it was found that the Re had to be above a threshold value ($R_\lambda > 30$ in the Jayesh & Warhaft experiment) before the exponential tails occurred. Moreover, these experimentalists recognized that the apparatus had to be ≥ 8 integral scales wide, or the tails are lost because of wall effects. It is therefore unsurprising that Thoroddsen et al (1998) (in grid experiments) and Overholt & Pope (1996) (in DNS) did not observe exponential tails, because their experimental or computational domain was too small, and that Kimura & Kraichnan (1993) and Rogers et al (1989) did not observe them (in their DNS) because the Re was too low (and possibly because their computational domain was too small also).

In a somewhat more complex experimental situation of turbulent pipe flow mixing, Guilkey et al (1997) observed scalar exponential tails, similar to those of Figure 13b. In their experiment there is a significant scale separation of the scalar and velocity fluctuations, such that the low-wave-number scalar fluctuations act as the imposed mean-scalar gradient, providing a similar situation to the grid experiment. Other numerical experiments (Jaberi et al 1996, Ching & Tu 1994) observe exponential tails in the presence of mean gradients, as well as under other conditions for which the relationship to real experiments is unclear.

Two broad points need to be made. First, it is now quite evident that the scalar signal need not be Gaussian, even in homogeneous turbulence for which the velocity field itself is Gaussian. The remarkable result is that theory and experiment show the existence of super-Gaussian (exponential) tails for a linear scalar gradient. This indicates departure from uniform mixing under the simplest of boundary conditions.

Second, this result is of more than academic significance. Figure 13b shows that the probability of a rare event, for example, at 4 standard deviations, is around

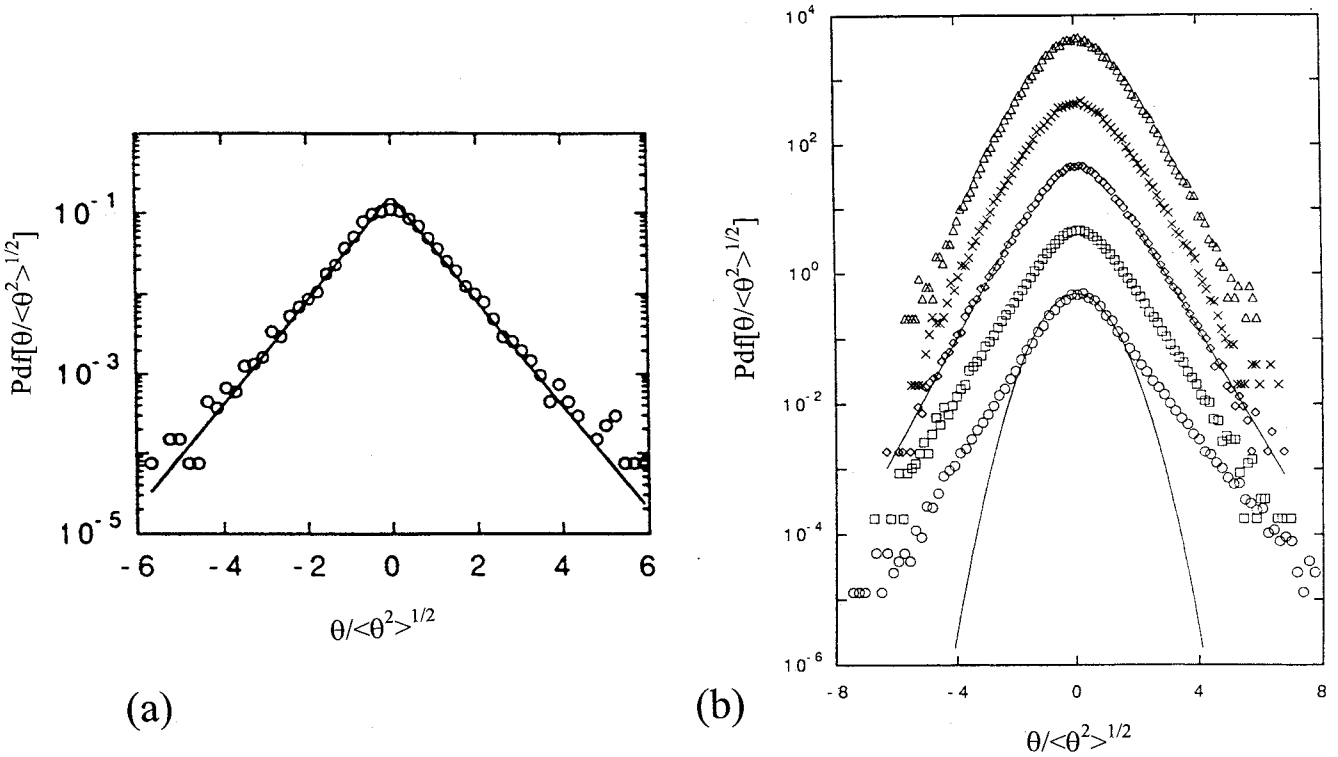

Figure 13 The probability density function (pdf) of the passive scalar signal, θ. (a) From Gollub et al (1991). (b) From Jayesh & Warhaft (1992) [see also Jayesh and Warhaft 1991]. Each pdf has been shifted one decade from the next lower one. The distance from the grid is $x/M = 36.4$ (*lowest curve*, compared with a Gaussian curve) to $x/M = 132.4$. The R_λ is 74.4 at $x/M = 62.4$.

10^3 higher than the value expected for a Gaussian distribution with the same variance. In the atmosphere, dispersion downwind from a point or area source of very small quantities of highly toxic substances can be harmful or deadly. Thus attention will have to be paid to the tails of the scalar pdf, which are at present assumed by pollution agencies to be Gaussian. Similarly, combustion and mixing both in the atmosphere and laboratory may be affected by the tails of the distribution.

6.2 The Scalar Variance, Flux, and Covariance

So far we have considered passive scalar statistics at a single position in the flow, without regard to their evolution. Most engineering problems require information on how the scalar variance and flux vary with position (and time). This is a large subject, compounded by the many variations in boundary and initial conditions of interest to the engineer. Here we summarize some of the more general aspects.

The way an excited system relaxes back to an equilibrium state is a general problem in mechanics. When stirring suddenly ceases in a fluid (or when a smooth velocity field passes through a grid), the question of how long the velocity fluctuations take to decay is central and unsolved (Batchelor 1953, for recent advances see George 1992, Speziale & Bernard 1992, Mohamed & LaRue 1990). If scalar fluctuations (in the absence of a mean gradient) are also induced at or near the turbulence-generating grid, at what rate does their variance decay? The governing equations are

$$U d\langle q^2\rangle/dx = -\langle\varepsilon\rangle \tag{13}$$

and

$$U \mathrm{d}\langle\theta^2\rangle/\mathrm{d}x = -\langle\varepsilon_\theta\rangle, \tag{14}$$

where $\langle q^2\rangle \equiv \frac{1}{2}[\langle u^2\rangle + \langle v^2\rangle + \langle w^2\rangle] \sim 3/2\,\langle u^2\rangle$ is the turbulence kinetic energy per unit mass.

Warhaft & Lumley (1978) showed that the decay rate of $\langle\theta^2\rangle$ is a function of the ratio of the initial velocity to scalar length scale (determined from the spectrum). As the initial length scale ratio was increased, so too was the decay rate of the scalar variance. They described their results in terms of the ratio of mechanical to thermal time scales $r \equiv \tau/\tau_\theta = (\langle q^2\rangle/\langle\varepsilon\rangle)/(\langle\theta^2\rangle/\langle\varepsilon_\theta\rangle)$, which varied from 0.9 to 2.4, depending on the wave number at which the thermal fluctuations were introduced. Further experiments (for ℓ_θ significantly less than ℓ) were done by Sreenivasan et al (1980) and, for both helium as well as temperature fluctuations, by Sirivat & Warhaft (1982). It might be thought that, far downstream, the turbulence would force r to some universal value. Warhaft (1984) shows that, even at 500-grid-mesh lengths, this does not occur. However, DNSs by Eswaran & Pope (1988) find that, after a long period, the thermal variance decay rate becomes independent of the initial conditions. There is also evidence of some relaxation from the initial value of r in the stochastic pair-dispersion model of Durbin (1982).

The problem is basic and needs to be resolved. The scalar field may be considered as the superposition of multiple-point or line sources (Durbin 1982, Warhaft 1984). At issue is how the variance from a line (or point) source evolves? What is the asymptotic value of $\langle\theta^2\rangle/T^2$? (Here T is the mean value of the scalar above ambient.) Headway has been made using particle dispersion theory (Durbin 1980, 1982, Lundgren 1981, Sawford & Hunt 1986, Stapountzis et al 1986, Thomson 1986, 1990, Borgas & Sawford 1994). In nondecaying flows, $\langle\theta^2\rangle/T^2$ tends to order 1 (Sawford et al 1985, Fackrell & Robins 1982), but in decaying grid turbulence the issue is far from settled (Warhaft 1984, Stapountzis et al 1986, Li & Bilger 1996).

The complexity arises because molecular diffusion and viscosity, as well as source size, play an important role even far from the source (Stapountzis et al 1986, Sawford & Hunt 1986, Borgas & Sawford 1996). It is properly addressed by means of Lagrangian dynamics, yet there is a lack of high-Re-data of Lagrangian measurements, and this impedes modeling attempts. For example, the Kolmogorov constant for acceleration variance is still poorly determined (e.g. Du et al 1995, Voth et al 1998) with estimates ranging from 3 to 7. Here there is a promise of progress in the near future, with the fast particle-tracking technique being developed by Bodenschatz's group (Voth et al 1998). There is also progress in this area from DNS (Yeung & Pope 1989).

The problem becomes a little simpler if a linear temperature profile is imposed on the grid turbulence (Corrsin 1952, Wiskind 1962). Here the mean profile forces the timescale ratio to a constant value (of ~ 1.5), irrespective of its initial value (Sirivat & Warhaft 1983, Budwig et al 1985), and success in modeling this flow has been achieved by using simple closures (e.g. Shih & Lumley 1986, Rogers et al 1989). Because there is a mean profile, there is a transverse heat flux, $\rho c_p\langle\theta v\rangle$. This is the simplest heat flux experiment that can be done, yet the Nusselt-Re number dependence is not well established. [The Nusslet number is the ratio of the total heat flux to the molecular heat flux and, for moderately high Re numbers, it can be estimated as $\langle\theta v\rangle/(k\mathrm{d}T/\mathrm{d}y)$, where k is the thermal conductivity.] In decaying grid turbulence Jayesh & Warhaft (1992) found that

$$\mathrm{Nu} = 0.73\mathrm{Re}_\ell^{0.88} \quad (60 \leq \mathrm{Re}_\ell \leq 1100), \tag{15}$$

where $\mathrm{Re}_\ell \equiv \langle u^2\rangle^{1/2}\ell/\nu$. In their shaking-grid experiments (also done with a linear temperature profile), Gollub et al (1991) found that

$$\mathrm{Nu} = 0.32\mathrm{Re}^{0.64} \quad (150 \leq \mathrm{Re} \leq 3000). \tag{16}$$

Here the Re was obtained from bulk parameters, and so the relationship to the turbulence Re_ℓ is not direct and may account for the differences in the exponent in the two experiments. Differences in the Re regimes and flow geometry may also play a role. More experiments are needed.

Because there is a heat flux, there is a cross-spectrum between θ and v, $F_{\theta v}(k_1)$. Dimensional arguments for $F_{\theta v}(k_1)$ [and for $F_{uv}(k_1)$, the Re stress spectrum in shear flow] indicate a $k^{-7/3}$ dependence (Lumley 1967). That the scaling suggests

a faster decrease with wave number for $F_{\theta v}(k_1)$ than for $F_\theta(k_1)$ is consistent with local isotropy, because θ and v (or u and v) should be uncorrelated at high wave numbers. Both Tavoularis & Corrsin (1981b) in homogeneous shear flow with a linear temperature profile and Mydlarski & Warhaft (1998a) in decaying grid turbulence show that the return to isotropy of $\langle \theta v \rangle$ is slower than that of $\langle uv \rangle$; that is, $F_{\theta v}(k_1)$ does not decrease as fast as $-7/3$. Mydlarski & Warhaft (1998a) attribute this to a low-Re-effect (although they do not see a significant change with the Re). There appear to be no high-Re-measurements to compare with the $F_{uv}(k_1)$ measurements of Saddoughi & Veeravalli (1994), who find good confirmation of the 7/3 law for the shear stress. The subject requires further attention because the available results may suggest that $F_{\theta v}(k_1)$ is being affected by small-scale anisotropy. Resolution of this issue is necessary for modeling of the scalar flux in such procedures as LES.

In turbulent mixing and reactions, the way in which two separate fluctuating scalars are correlated and how the correlation evolves are of paramount importance. For example, for a one-step irreversible second-order chemical reaction between chemical species A and B in an isothermal flow (A + B → C + D), the diffusion equation for the mean concentration $\langle C \rangle$, of A or B is (Mao & Toor 1971, Bilger 1989, Komori et al 1991a)

$$\partial\langle C\rangle/\partial t + U_i \partial\langle C\rangle/\partial x_i = \partial[\kappa(\partial\langle C\rangle/\partial x_i) - \langle u_i c\rangle]/\partial x_i - \mathbf{K}[\langle C_A\rangle\langle C_B\rangle + \langle c_A c_B\rangle], \quad (17)$$

where C and c are the instantaneous and fluctuating concentrations, κ is the molecular diffusivity and **K** is the chemical-reaction-rate constant. The way c_A and c_B are correlated can change the sign of the mean chemical rate term (second term on the right). This correlation is expressed in the normal way as $\rho \equiv \langle c_A c_B\rangle/(\langle c_A^2\rangle^{1/2} \langle c_B^2\rangle^{1/2})$ or as $\alpha \equiv \langle c_A c_B\rangle/(\langle C_A\rangle\langle C_B\rangle)$, where α is called the segregation coefficient. If $\alpha = -1$, there is no molecular mixing. A study of α and ρ has been made by Komori et al (1991a) for non-premixed reacting flows with a Lagrangian stochastic model, and DNS studies of two-scalar mixing without reaction, including the evolution of their joint pdf, have been performed by Juneja & Pope (1996). Both ρ and α are strongly dependent on the Re, Schmidt number, and Damköhler number (the ratio of the turbulence time scale to the reaction rate time scale) and also vary widely within a particular flow. For example for two plumes introduced separately into a fluid, Warhaft (1984) shows that $\rho \sim -1$ close to the sources, where the plumes are being flapped in synchronism by the turbulence, to $+1$ far downstream, where the plumes have mixed. These results have been confirmed in the boundary-layer measurements of Sawford et al (1985). α too shows wide variation (Bennani et al 1985, Komori et al 1991b, Li & Bilger 1996, Tong & Warhaft 1995). A systematic study of different flows is still lacking, and there is controversy even concerning the sign of α in some flows (Bilger et al 1985,

Komori et al 1991a). Measurements of α for atmospheric mixing, in which accurate knowledge of reactions involving HNO_3, O_3 and other species are badly needed, are practically nonexistent (see e.g. Pyle & Zavody 1990).

Finally, for reactions more complex than one-step second-order (Equation 17), turbulence information, in addition to the covariance itself, is needed to model the reaction rates (Bilger 1989). Here knowledge of the fine-scale structure itself may be required. This is also the case for the mixing of two passive scalars with different diffusivities (e.g. Yeung & Pope 1993). Problems such as these provide further motivation for the study of small-scale dynamics discussed in the earlier parts of this review.

7. SCHMIDT NUMBER EFFECTS

Much of the visual information concerning passive scalars has come from flow imaging of dye in liquids (e.g. Buch & Dahm 1996, Karasso & Mungal 1996, Catrakis & Dimotakis 1996, Williams et al 1997, Huq & Britter 1995). These experiments tend to confirm the in situ point measurements elaborated in this review, that is, that there are sharp gradient sheets or fronts in the scalar field that we have characterized as ramp-cliff structures. For these liquid experiments the Schmidt number Sc [$\equiv \nu/\kappa$ where κ is the molecular diffusivity of the scalar (usually a fluorescent dye)] is high, of order 10^3. This does not change inertial-range characteristics. For example, Miller & Dimotakis (1996) show that the scalar spectra for Sc $\sim$ 2000 in a jet follow a similar evolution with Re to that observed in gas flow experiments (e.g. Dowling & Dimotakis 1990); that is, the magnitude of the spectrum slope is significantly less than 5/3, tending to 5/3 only at very high Re (as in Figure 4).

Yet for high Sc, there are two dissipation scales or wave numbers (Tennekes & Lumley 1972): the Kolmogorov wave number for the velocity field $k_\eta \equiv (\varepsilon/\nu^3)^{1/4}$ and the Batchelor wave number for the scalar $k_{\eta\theta} \equiv (\varepsilon/\nu\kappa^2)^{1/4}$. For high Sc, $k_{\eta\theta} > k_\eta$, and the velocity fluctuations are dissipated at lower wave numbers than the scalar fluctuations. In the wave number interval $k_\eta < k < k_{\eta\theta}$ (known as the viscous-convective range), the random velocity field varies linearly with position, and Batchelor (1959) predicted that the scalar spectrum should display a k^{-1} dependence. The experimental evidence has been elusive, and here we mention the most recent results.

In their turbulent jet experiment, Miller & Dimotakis (1996), paying particular attention to probe resolution and the signal-to-noise ratio problems that have plagued earlier experiments, find no k^{-1} scaling region, despite a relatively high Sc ($\sim$2000). In an altogether different experimental set up, Williams et al (1997) studied passive scalar mixing in magnetically forced two-dimensional turbulence. Here too the Sc was 2000. They found that the scalar spectrum fell strongly below k^{-1}, again inconsistent with the Batchelor prediction. Williams et al (1997) surmise that intermittency in the velocity field may have affected their results. We

note that in both experiments, the wave number range of the viscous-convective range at these Sc numbers is <1.5 decades. Our knowledge of inertial-range spectra would be poor if this was the maximum wave number range at our disposal. There is strong reason that the k^{-1} region should exist (Kraichnan 1968, Holzer & Siggia 1994), and more experiments are needed.

8. CONCLUDING REMARKS

The study of passive scalars is exciting because the richness of the new phenomena was not easily envisioned. That a passive additive, obeying a linear equation, displays characteristics so different from those of the advecting velocity field is remarkable. The existence of exponential tails in the scalar signal while the velocity is Gaussian; the strong inertial subrange intermittency in the scalar, which occurs at low Re where intermittency in the velocity field is absent; the contrast between the scalar and velocity spectra; and the anisotropy, both at dissipation and inertial scales, are all departures from expected behavior. They must play a determining role in mixing, dispersion, and reactions, and the way we model them. Thus the new findings provide intellectual challenge and yet are of practical importance.

The issue of the scalar anistropy has been particularly emphasized. Our focus has been on the skewness (third-moment) statistics, particularly in the inertial range. Not only is it a violation of the cornerstone of turbulence theory—the notion of local isotropy—but we believe that its study provides a program toward understanding the intermittency problem itself. The approach outlined in Section 4 indicates the direct link between the large and small scales and thus the inadequacy of a simple step-by-step cascade model. The three-point correlations entice us to look at the scalar field in new ways. We believe that the approach used for the scalar problem could also shed light on the inertial- and dissipation-range velocity structure, where measurements and computations at moderate Re have shown that skewness on the order of 1 is also observed, in violation of inertial-range isotropy (Tavoularis & Corrsin 1981b, Pumir & Shraiman 1995, Pumir 1996b, Garg & Warhaft 1998).

Finally, it should be apparent from this review that the subject of passive scalars is vast. My focus has inevitably been on work with which I have been involved, and there are omissions that may appear to some as egregious. There has been little mention of the overall budget of scalar variance and heat flux in the standard laboratory flows and nothing about complex flows [a topic last reviewed by Hunt (1985)]. The viewpoint has been experimental, and even here little has been said about the exciting diagnostic tools that are being developed. The subject of fractals, which may well provide new interpretations of the data (Sreenivasan & Meneveau 1986, Prasad et al 1988, Sreenivasan et al 1989, Frederiksen et al 1997, Miller & Dimotakis 1991, Villermaux & Gagne 1994), has not been addressed. We note, curiously, that this is the first annual review of the

subject of passive scalars. Let us hope it will not be too long before this vital topic will again be addressed from other perspectives.

ACKNOWLEDGMENTS

Foremost, I thank Eric Siggia, who has confirmed my belief that the theoretician can make provocative and verifiable predictions, even in the difficult subject of turbulence. He, Boris Shraiman, and Alan Pumir have provided the stimulus for much of the recent work reported here. I also thank my students Laurent Mydlarski, Chenning Tong, Sandeep Garg and the late Jayesh. Thoughtful comments on a first draft were made by O. Boratav, J. L. Lumley, L. Mydlarski, M. Nelkin, S. B. Pope, B. I. Shraiman, E. D. Siggia, and A. Tsinober. Deanna Spoth generously assisted me in the production of the manuscript. Finally I thank the Department of Energy, Division of Basic Energy Sciences, for their sustained support over the past decade.

LITERATURE CITED

Anselmet F, Djeridi H, Fluachier L. 1994. Joint statistics of a passive scalar and its dissipation in turbulent flows. *J. Fluid Mech.* 280:173–97

Anselmet F, Gagne Y, Hopfinger EJ, Antonia RA. 1984. High-order velocity structure functions in turbulent shear flows. *J. Fluid Mech.* 140:63–89

Antonia RA, Chambers AJ, Britz D, Browne LW. 1986. Organized structures in a turbulent plane jet: topology and contribution to momentum and heat transport. *J. Fluid Mech.* 172:211–29

Antonia RA, Hopfinger EJ, Gagne Y, Anselmet F. 1984. Temperature structure functions in turbulent shear flows. *Phys. Rev. A* 30:2704–7

Antonia RA, Van Atta CW. 1975. On the correlation between temperature and velocity dissipation fields in a heated turbulent jet. *J. Fluid Mech.* 67:273–88

Antonia RA, Van Atta CW. 1978. Structure functions of temperature fluctuations in turbulent shear flows. *J. Fluid Mech.* 84:561–80

Batchelor GK. 1953. *The Theory of Homogeneous Turbulence.* Cambridge Univ. Press

Batchelor GK. 1959. Small-scale variation of convected quantities like temperature in a turbulent field. Part 1. General discussion and the case of small conductivity. *J. Fluid Mech.* 5:113

Bennani A, Gence JN, Mathieu J. 1985. The influence of a grid-generated turbulence on the development of chemical reactions. *AIChE J.* 31:1157–66

Benzi R, Ciliberto S, Tripiccione R, Baudet C, Massaioli F, Succi S. 1993. Extended self-similarity in turbulent flows. *Phys. Rev. E* 48:R29–R32

Bilger RW. 1989. Turbulent diffusion flames. *Annu. Rev. Fluid Mech.* 21:101–35

Bilger RW, Mudford NR, Atkinson JD. 1985. Comments on turbulent effects on the chemical reaction for a jet in a nonturbulent stream and for a plume in a grid-generated turbulence. *Phys. Fluids* 28:3175–77

Boratav O, Eden A, Erzan A, eds. 1997. *Turbulence Modeling and Vortex Dynamics.* Berlin: Springer-Verlag

Boratav O, Pelz R. 1998. Coupling between anomalous velocity and passive scalar increments in turbulence. *Phys. Fluids* 10:2122–24

Borgas MS, Sawford BL. 1994. A family of stochastic models for two-particle dispersion in isotropic homogeneous stationary turbulence. *J. Fluid Mech.* 279:69–99

Borgas MS, Sawford BL. 1996. Molecular diffusion and viscous effects on concentration statistics in grid turbulence. *J. Fluid Mech.* 324:25–54

Buch KA, Dahm WJA. 1996. Experimental study of the fine-scale structure of conserved scalar mixing in turbulent shear flows. Part 1. Sc $\gg$ 1. *J. Fluid Mech.* 317:21–71

Budwig R, Tavoularis S, Corrsin S. 1985. Temperature fluctuations and heat flux in grid generated isotropic turbulence with streamwise and transverse mean-temperature gradients. *J. Fluid Mech.* 153:441–60

Castaing B, Gunaratne G, Helsot F, Kadanoff L, Libchaber A, et al. 1989. Scaling of hard thermal turbulence in Rayleigh-Bernard convection. *J. Fluid Mech.* 204:1–30

Catrakis HJ, Dimotakis PE. 1996. Mixing in turbulent jets: scalar measures and isosurface geometry. *J. Fluid Mech.* 317:369–406

Chambers AJ, Antonia RA. 1984. Atmospheric estimates of power law exponents μ and μ_θ. *Boundary-Layer Met.* 28:343–52

Champagne FH. 1978. The fine-scale structure of the turbulent velocity field. *J. Fluid Mech.* 86:67–108

Chen S, Kraichnan RH. 1998. Simulations of a randomly advected passive scalar field. *Phys. Fluids* 10:2867–84

Chertkov M, Falkovich G, Kolokolov I, Lebeder V. 1995. Normal and anomalous scaling of the 4th order correlation-function of a randomly advected passive scalar. *Phys. Rev.* E 52:4924–41

Ching ESC, Tu Y. 1994. Passive scalar fluctuations with and without a mean gradient: a numerical study. *Phys. Rev.* E 49:1278–82

Corrsin S. 1951. On the spectrum of isotropic temperature fluctuations in isotropic turbulence. *J. Appl. Phys.* 22:469–73

Corrsin S. 1952. Heat transfer in isotropic turbulence. *J. Appl. Phys.* 23:113–18

Dowling DR, Dimotakis PE. 1990. Similarity of the concentration field of gas-phase turbulent jets. *J. Fluid Mech* 218:109–41

Du S, Sawford BL, Wilson DJ. 1995. Estimation of the Kolmogorov constant (C_0) for the Lagrangian structure function, using a second-order Lagrangian model of grid turbulence. *Phys. Fluids* 7:3083–90

Durbin PA. 1980. A stochastic model of two-particle dispersion and concentration fluctuations in homogeneous turbulence. *J. Fluid Mech.* 100:279–302

Durbin PA. 1982. Analysis of the decay of temperature fluctuations in isotropic turbulence. *Phys. Fluids* 25:1328–32

Eswaran V, Pope SB. 1988. Direct numerical simulations of the turbulent mixing of a passive scalar. *Phys. Fluids* 31:506–20

Fackrell JE, Robins AG. 1982. Concentration fluctuations and fluxes in plumes from point sources in a turbulent boundary layer. *J. Fluid Mech.* 117:1–26

Frederiksen RD, Werner JA, Dahm JA, Dowling DR. 1997. Experimental assessment of fractal scale similarity in turbulent flows. Part 3. Multifractal scaling. *J. Fluid Mech.* 338:127–155

Freymuth P, Uberoi MS. 1971. Structure of temperature fluctuations in the wake behind a cylinder. *Phys. Fluids* 14:2574–80

Frisch U. 1995. *Turbulence: the Legacy of A.N. Kolmogorov.* Cambridge, U.K.: Cambridge Univ. Press

Frisch U, Mazzino A, Vergassola M. 1998. Intermittency in passive scalar advection. *Phys. Rev. Lett.* 80:5532–5

Galperin B, Orszag SA. 1993. *Large eddy simulation of complex engineering and geophysical flows.* Cambridge, UK: Cambridge Univ. Press

Garg S, Warhaft Z. 1998. On small scale statistics in a simple shear flow. *Phys. Fluids* 10:662–73

Gawedzki K, Kupiainen A. 1995. Anomalous scaling of the passive scalar. *Phys. Rev. Lett.* 75:3834–37

George WK. 1992. The decay of homogeneous isotropic turbulence. *Phys. Fluids A* 4: 1492–1509

Gibson CH, Friehe CA, McConnell SO. 1977. Skewness of temperature derivatives in turbulent shear flows. *Phys. Fluids Suppl.* 20:156–67

Gibson CH, Stegen GR, Williams RW. 1970. Statistics of the fine structure of turbulent velocity and temperature fields measured at high Reynolds number. *J. Fluid Mech.* 41:153–67

Gollub JP, Clarke J, Gharib M, Lane B, Mesquita ON. 1991. Fluctuations and transport in a stirred fluid with a mean gradient. *Phys. Rev. Lett.* 67:3507–10

Guilkey JE, Kerstein AR, McMurtry PS, Klewicki JC. 1997. Long-tailed probability distributions in turbulent-pipe-flow mixing. *Phys. Rev. E* 56:1753–58

Hinze JO. 1975. *Turbulence.* New York: McGraw-Hill

Holzer M, Pumir A. 1993. Simple models of non-Gaussian statistics for a turbulently advected passive scalar. *Phys. Rev. E* 47:202–19

Holzer M, Siggia ED. 1994. Turbulent mixing of a passive scalar. *Phys. Fluids* 6:1820–37

Hunt JCR. 1985. Turbulent diffusion from sources in complex flows. *Annu. Rev. Fluid Mech.* 17:447–86

Huq P, Britter RE. 1995. Mixing due to grid-generated turbulence of a two-layer scalar profile. *J. Fluid Mech.* 285:17–40

Jaberi FA, Miller RS, Madnia CK, Givi P. 1996. Non-Gaussian scalar statistics in homogeneous turbulence. *J. Fluid Mech.* 313:241–82

Jayesh, Tong C, Warhaft Z. 1994. On temperature spectra in grid turbulence. *Phys. Fluids* 6:306–12

Jayesh, Warhaft Z. 1991. Probability distribution of a passive scalar in grid-generated turbulence. *Phys. Rev. Lett.* 67:3503–6

Jayesh, Warhaft Z. 1992. Probability distribution, conditional dissipation, and transport of passive temperature fluctuations in grid generated turbulence. *Phys. Fluids A* 4:2292–307

Juneja A, Pope SB. 1996. A DNS study of turbulent mixing of two passive scalars. *Phys. Fluids* 8:2177–84

Karasso PS, Mungal MG. 1996. Scalar mixing and reaction in plane liquid shear layers. *J. Fluid Mech.* 323:23–63

Kerstein AR. 1991. Linear-eddy modeling of turbulent transport. Part 6. Microstructure of diffusive scalar mixing fields. *J. Fluid Mech.* 231:361–94

Kerstein AR, McMurtry PA. 1994. Mean-field theories of random advection. *Phys. Rev. E* 49:474–82

Kimura Y, Kraichnan RH. 1993. Statistics of an advected passive scalar. *Phys. Fluids A* 5:2264–77

Kolmogorov AN. 1962. A refinement of previous hypotheses concerning the local structure of turbulence in a viscous incompressible fluid at high Reynolds number. *J. Fluid Mech.* 13:82–85

Kolmogrov AN. 1941. The local structure of turbulence in incompressible viscous fluid for very large Reynolds number, *Dokl. Akad. Nauk SSSR* 30:9–13

Komori S, Hunt JCR, Kanzaki T, Murakami Y. 1991a. The effects of turbulent mixing on the correlation between two species and on concentration fluctuations in nonpremixed reacting flows. *J. Fluid Mech.* 228:629–59

Komori S, Kanzaki T, Murakami Y. 1991b. Simultaneous measurements on instantaneous concentrations of two reacting species in a turbulent flow with a rapid reaction. *Phys. Fluids A* 3:507–10

Korchashkin NN. 1970. The effect of fluctuations of energy dissipation and temperature dissipation on locally isotropic turbulent fields. *Izv. Oceanic Phys.* 6:947–49

Kraichnan RH. 1968. Small-scale structure of a scalar field convected by turbulence. *Phys. Fluids* 11:945–63

Kraichnan RH. 1994. Anomalous scaling of a randomly advected passive scalar. *Phys. Rev. Lett.* 72:1016

L'vov V, Procaccia I. 1997. Hydrodynamic turbulence: a 19th century problem with a challenge for the 21st century. See Boratav et al 1997, pp. 1–16

Lane BR, Mesquita ON, Meyers SR, Gollub JP. 1993. Probability distributions and thermal transport in a turbulent grid flow. *Phys. Fluids A* 5:2255–63

Lesieur M. 1997. *Turbulence in Fluids.* Dordrecht: Kluwer. 515 pp.

Li JD, Bilger RW. 1996. The diffusion of conserved and reactive scalars behind line sources in homogeneous turbulence. *J. Fluid Mech.* 318:339–72

Lohse D, Müller-Groeling A. 1996. Anisotropy and scaling corrections in turbulence. *Phys. Rev. E* 54:395–405

Lumley JL. 1967. Similarity and the turbulent energy spectrum. *Phys. Fluids* 10:855–58

Lundgren TS. 1981. Turbulent pair dispersion and scalar diffusion. *J. Fluid Mech.* 111:27–57

Ma B, Warhaft Z. 1986. Some aspects of the thermal mixing layer in grid turbulence. *Phys. Fluids* 29:3114–20

Mao KW, Toor HL. 1971. Second-order chemical reactions with turbulent mixing. *Ind. Eng. Chem. Fundam.* 10:192–97

Meneveau C, Sreenivasan KR, Kailasnath P, Fan MS. 1990. Joint multifractal measures: theory and applications to turbulence. *Phys. Rev. A* 41:894–913

Mestayer PG. 1982. Local isotropy and anisotropy in a high-Reynolds number turbulent boundary layer. *J. Fluid Mech.* 125:475–503

Mestayer PG, Gibson CH, Coantic MF, Patel AS. 1976. Local anisotropy in heated and cooled turbulent boundary layers. *Phys. Fluids* 19:1279–87

Mi J, Antonia A. 1995. Joint statistics between temperature and its dissipation rate components in a round jet. *Phys. Fluids* 7:1665–73

Miller PL, Dimotakis PE. 1991. Stochastic geometric properties of scalar interfaces in turbulent jets. *Phys. Fluids A* 3:168–77

Miller PL, Dimotakis PE. 1996. Measurements of scalar power spectra in high Schmidt number turbulent jets. *J. Fluid Mech.* 308:129–46

Mohamed MS, LaRue JC. 1990. The decay power law in grid-generated turbulence. *J. Fluid Mech.* 219:195–214

Monin AS, Yaglom AM. 1975. *Statistical Fluid Mechanics,* Vol. 2. Cambridge, MA: MIT Press

Mydlarski L, Pumir A, Shraiman BI, Siggia ED, Warhaft Z. 1998. Structures and multipoint correlators for turbulent advection: predictions and experiments. *Phys. Rev. Lett.* 81:4373–76

Mydlarski L, Warhaft Z. 1996. On the onset of high-Reynolds number grid-generated wind tunnel turbulence. *J. Fluid Mech.* 320:331–68

Mydlarski L, Warhaft Z. 1998a. Passive scalar statistics in high-Péclet-number grid turbulence. *J. Fluid Mech.* 358:135–75

Mydlarski L, Warhaft Z. 1998b. Three-point statistics and the anisotropy of a turbulent passive scalar. *Phys. Fluids.* 10:2885–94

Nelkin M. 1994. Universality and scaling in fully developed turbulence. *Adv. Phys.* 43:143–81

O'Brien EE, Jiang T. 1991. The conditional dissipation rate of an initially binary scalar in homogeneous turbulence. *Phys. Fluids A* 3:3121–23

Obukhov AM. 1962. Some specific features of atmospheric turbulence. *J. Fluid Mech.* 13:77–81

Obukhov AM. 1949. Structure of the temperature field in turbulent flows. *Izv. Akad. Nauk. SSSR, Geogr. Geofiz.*, 13:58–69

Overholt MR, Pope SB. 1996. Direct numerical simulation of a passive scalar with imposed mean gradient in isotropic turbulence. *Phys. Fluids* 8:3128–48

Pope SB, Ching ESC. 1993. Stationary probability density functions: an exact result. *Phys. Fluids A* 5:1529–31

Prasad RR, Meneveau C, Sreenivasan KR. 1988. Multifractal nature of the dissipation field of passive scalars in fully turbulent flow. *Phys. Rev. Lett.* 61:74–77

Pumir A. 1994. A numerical study of the mixing of a passive scalar in three dimensions in the presence of a mean gradient. *Phys. Fluids* 6:2118–312

Pumir A. 1996a. Anomalous scaling behavior of a passive scalar in the presence of a mean gradient. *Europhys. Lett.* 34:25–29

Pumir A. 1996b. Turbulence in homogeneous shear flows. *Phys. Fluids* 8:3112–27

Pumir A. 1997. Determination of the 3-point correlation function of a passive scalar in the presence of a mean gradient. *Europhys. Lett.* 37:529–34

Pumir A. 1998. Structure of the three-point correlation function of passive scalar in the presence of a mean gradient. *Phys. Rev. E* 57:2914–29

Pumir A, Shraiman BI. 1995. Persistent small scale anisotropy in homogeneous shear flows. *Phys. Rev. Lett.* 75:3114–17

Pumir A, Shraiman B, Siggia ED. 1991. Exponential tails and random advection. *Phys. Rev. Lett.* 3:2838–40

Pyle JA, Zavody AM. 1990. The modelling problems associated with spatial averaging. *Q. J. R. Meteorol. Soc.* 116:753–66

Rogers MM, Mansour NN, Reynolds WC. 1989. An algebraic model for the turbulent flux of a passive scalar. *J. Fluid Mech.* 203:77–101

Ruiz-Chavarria G, Baudet C, Ciliberto S. 1996. Scaling laws and dissipation scale of a passive scalar in fully developed turbulence. *Physica D* 99:369–80

Saddoughi SG, Veeravalli SV. 1994. Local isotropy in turbulent boundary layers at high Reynolds number. *J. Fluid Mech.* 268:333–72

Sahay A, O'Brien EE. 1993. Uniform mean scalar gradient in grid turbulence: conditioned dissipation and production. *Phys. Fluids A* 5:1076–78

Sawford BL, Frost CC, Allan TC. 1985. Atmospheric boundary-layer measurements of concentration statistics from isolated and multiple sources. *Boundary Layer Meteorol.* 31:249–68

Sawford BL, Hunt JCR. 1986. Effects of turbulence structure, molecular diffusion and source size on scalar fluctuations in homogeneous turbulence. *J. Fluid Mech.* 165:373–400

Shih T, Lumley JL. 1986. Influence of timescale ration on scalar flux relaxation: modeling Sirivat & Warhaft's homogeneous passive scalar fluctuations. *J. Fluid Mech.* 162:211–22

Shraiman BI, Siggia ED. 1994. Lagrangian path integrals and fluctuations in random flow. *Phys. Rev. E* 49:2912–27

Shraiman BI, Siggia ED. 1995. Anomalous scaling of a passive scalar in turbulent flow. *C. R. Acad. Sci., Ser. IIb.* 321:279–84

Shraiman BI, Siggia ED. 1996. Symmetry and scaling of turbulent mixing. *Phys. Rev. Lett.* 77:2463–66

Shraiman BI, Siggia ED. 1999. Scalar turbulence. *Nature.* Submitted

Siggia ED. 1994. High Rayleigh number convection. *Annu. Rev. Fluid Mech.* 26:137–68

Sinai YG, Yakhot V. 1989. Limiting probability distributions of a passive scalar in a random velocity field. *Phys. Rev. Lett.* 63: 1962–65

Sirivat A, Warhaft Z. 1982. The mixing of passive helium and temperature fluctuations in grid turbulence. *J. Fluid Mech.* 120:475–504

Sirivat A, Warhaft Z. 1983. The effect of a passive cross-stream temperature gradient on the evolution of temperature variance and heat flux in grid turbulence. *J. Fluid Mech.* 128:323–46

Speziale CG, Bernard PS. 1992. The energy decay in self-preserving isotropic turbulence revisited. *J. Fluid Mech.* 241:645–67

Sreenivasan KR. 1991. On local isotropy of passive scalars in turbulent shear flows. *Proc. R. Soc. London. Ser. A* 434:165–82

Sreenivasan KR. 1995. On the universality of the Kolmogorov constant. *Phys. Fluids* 7:2778–84

Sreenivasan KR. 1996. The passive scalar spectrum and the Obukhov-Corrsin constant. *Phys. Fluids* 8:189–96

Sreenivasan KR, Antonia RA. 1977. Skewness of temperature derivatives in turbulent shear flows. *Phys. Fluids* 20:1986–88

Sreenivasan KR, Antonia RA. 1997. The phenomenology of small-scale turbulence. *Annu. Rev. Fluid Mech.* 29:435–72

Sreenivasan KR, Antonia RA, Britz D. 1979. Local isotropy and large structures in a heated turbulent jet. *J. Fluid Mech.* 94:745–75

Sreenivasan KR, Antonia RA, Danh HQ. 1977. Temperature dissipation fluctuations in a turbulent boundary layer. *Phys. Fluids* 20:1238–49

Sreenivasan KR, Meneveau C. 1986. The fractal facets of turbulence. *J. Fluid Mech.* 173:357–89

Sreenivasan KR, Ramshankar R, Meneveau C. 1989. Mixing, entrainment and fractal dimensions of surfaces in turbulent flows. *Proc. R. Soc. London Ser. A* 421:79–108

Sreenivasan KR, Tavoularis S, Henry R, Corrsin S. 1980. Temperature fluctuations and scales in grid-generated turbulence. *J. Fluid Mech.* 100:597–621

Stapountzis H, Sawford BL, Hunt JCR, Britter RA. 1986. Structure of the temperature field downwind of a line source in grid turbulence. *J. Fluid Mech.* 165:401–24

Stewart RW. 1969. Turbulence and waves in stratified atmosphere. *Radio Sci.* 4:1269–78

Stolovitzky G, Kailasnath P, Sreenivasan KR. 1995. Refined similarity hypotheses for passive scalars mixed by turbulence. *J. Fluid Mech.* 297:275–91

Tatarskii VI, Dubovikov MM, Praskovsky AA, Karyakin MY. 1992. Temperature fluctuation spectrum in the dissipation range for statistically isotropic turbulent flow. *J. Fluid Mech.* 238:683–98

Tavoularis S, Corrsin S. 1981a. Experiments in nearly homogeneous turbulent shear flow with a uniform mean temperature gradient. Part 1. *J. Fluid Mech.* 104:311–47

Tavoularis S, Corrsin S. 1981b. Experiments in nearly homogeneous turbulent shear flow with a uniform mean temperature gradient. Part 2. The fine structure. *J. Fluid Mech.* 104:349–67

Tennekes H, Lumley JL. 1972. *A First Course in Turbulence.* Cambridge, MA: MIT Press 300 pp.

Thomson DJ. 1990. A stochastic model for the motion of particle pairs in isotropic high-Reynolds number turbulence, and its application to the problem of concentration variance. *J. Fluid Mech.* 210:113–53

Thomson DJ. 1986. On the relative dispersion of two particles in homogeneous stationary turbulence and the implications for the size of concentration fluctuations at large times. *Q. J. R. Met. Soc.* 112:890–94

Thoroddsen ST, Van Atta CW. 1996. Experiments on density-gradient anisotropies and scalar dissipation of turbulence in a stably stratified fluid. *J. Fluid Mech.* 322:383–409

Thoroddsen ST, Van Atta CW, Yampolsky JS. 1998. Experiments on homogeneous turbulence in an unstable stratified fluid. *Phys. Fluids* 10:3155–67

Tong C, Warhaft Z. 1994. On passive scalar derivative statistics in grid turbulence. *Phys. Fluids* 6:2165–76

Tong C, Warhaft Z. 1995. Passive scalar dispersion and mixing in a turbulent jet. *J. Fluid Mech.* 292:1–38

Van Atta CW. 1991. Local isotropy of the smallest scales of turbulent scalar and velocity fields. *Proc. R. Soc. London Ser. A* 434:139–47

Van Atta CW. 1971. Influence of fluctuations in local dissipation rates on turbulent scalar characteristics in the inertial subrange. *Phys. Fluids* 14:1803–4

Villermaux E, Gagne Y. 1994. Line dispersion in homogeneous turbulence: stretching fractal dimensions, and micromixing. *Phys. Rev. Lett.* 73:252–55

Voth GA, Satyanarayan K, Bodenschatz E. 1998. Lagrangian acceleration measurements at large Reynolds numbers. *Phys. Fluids* 10:2268–80

Warhaft Z. 1984. The interference of thermal fields from line sources in grid turbulence. *J. Fluid Mech.* 144:363–87

Warhaft Z, Lumley JL. 1978. An experimental study of the decay of temperature fluctuations in grid-generated turbulence. *J. Fluid Mech.* 88:659–84

Williams BS, Marteau D, Gollub JP. 1997. Mixing of passive scalar in magnetically forced two-dimensional turbulence. *Phys. Fluids* 9:2061–80

Wiskind HK. 1962. A uniform gradient turbulent transport experiment. *J. Geophys. Res.* 67:3033–48

Wyngaard JC. 1971. Spatial resolution of a resistance wire temperature sensor. *Phys. Fluids* 14:2052–54

Yaglom AM. 1949. On the local structure of a temperature field in a turbulent flow. *Dokl. Akad. Nauk. SSSR* 69:743–46

Yeh TT, Van Atta CW. 1973. Spectral transfer of scalar velocity fields in heated-grid turbulence. *J. Fluid Mech.* 58:233–61

Yeung PK, Pope SB. 1993. Differential diffusion of passive scalars in isotropic turbulence. *Phys. Fluids A* 5:2467–78

Yeung PK, Pope SB. 1989. Lagrangian statistics from direct numerical simulations of isotropic turbulence. *J. Fluid Mech.* 207:531–86

Zeldovich Ya-B, Molchanov SA, Ruzmaikin AA, Sokoloff DD. 1988. Intermittency, diffusion and generation in a nonstationary random medium. *Sov. Sci. Rev. C. Math. Phys.* 7:1–110

Zhu U, Antonia RA, Hosokawa I. 1995. Refined similarity hypotheses for turbulent velocity and temperature fields. *Phys. Fluids* 7:1637–48

Annual Review of Fluid Mechanics
Volume 32, 2000

CONTENTS